# PSECMAC Intelligent Insulin Schedule for Diabetic Blood Glucose Management Under Non Meal Announcement

*S. D. Teddy*[1], *C. Quek*[2]*, *E. M-K. Lai*[3] *and A. Cinar*[4]

***Contact Author:** Dr. Chai Quek

**Insitutions:**

[1]Data Mining Department, Institute for Infocomm Research, 1 Fusionopolis Way, #21-01 Connexis, Singapore 138632

[2]Center for Computational Intelligence, School of Computer Engineering, Nanyang Technological University, Block N4 #2A-32, Nanyang Avenue, Singapore 639798

[3]Institute of Information Sciences and Technology, Massey University, Wellington, New Zealand

[4]Department of Chemical and Biological Engineering, Illinois Institute of Technology, 10 West 33rd Street, Chicago, Illinois 60616

**Submitted to:** IEEE Transactions on Neural Networks

**Date of Submission:** October 2008

**Emails:**
[1]sdteddy@i2r.a-star.edu.sg
[2]ashcquek@ntu.edu.sg
[3]e.lai@massey.ac.nz
[4]cinar@iit.edu

**Tel/Fax:** (+65) 6790 4926 / (+65) 6792 6559

**Keywords:** diabetes, insulin therapy, intelligent insulin schedule, no meal announcement, PSECMAC

# PSECMAC Intelligent Insulin Schedule for Diabetic Blood Glucose Management Under Non Meal Announcement

S. D. Teddy[1], C. Quek[2]*, E. M-K. Lai[3] and A. Cinar[4]

[1]sdteddy@i2r.a-star.edu.sg, [2]ashcquek@ntu.edu.sg, [3]e.lai@massey.ac.nz, [4]cinar@iit.edu

---

## Abstract

Therapeutically, the closed-loop blood glucose-insulin regulation paradigm via a controllable insulin pump offers a potential solution to the management of diabetes. However, the development of such a closed-loop regulatory system to date has been hampered by two main issues. They are: (1) the limited knowledge on the complex human physiological process of glucose-insulin metabolism that prevents a precise modeling of the biological blood glucose control loop; and (2) the vast metabolic biodiversity of the diabetic population due to varying exogneous and endogenous disturbances such as food intake, exercise, stress and hormonal factors, etc. In addition, current attempts of closed-loop glucose regulatory techniques generally require some form of prior meal announcement and this constitutes a severe limitation to the applicability of such systems. In this paper, we present a novel intelligent insulin schedule based on the PSECMAC associative learning memory model that emulates the healthy human insulin response to food ingestion. The proposed PSECMAC intelligent insulin schedule requires no prior meal announcement and delivers the necessary insulin dosage based only on the observed blood glucose fluctuations. Using a simulated healthy subject, the proposed PSECMAC insulin schedule is demonstrated to be able to accurately capture the complex human glucose-insulin dynamics and robustly addresses the intra-person metabolic variability. Subsequently, the PSECMAC intelligent insulin schedule is employed on a group of Type-1 diabetic patients to regulate their impaired blood glucose levels. Preliminary simulation results are highly encouraging. The work reported in this paper represents a major paradigm shift in the management of diabetes where patient compliance is poor and the need for prior meal announcement under current treatment regimes poses a significant challenge to an active lifestyle.

## 1 Introduction

Diabetes is a chronic disease where the body is unable to properly and efficiently regulate the use and storage of glucose in the blood, leading to prolonged periods of high (hyperglycemia) or low (hypoglycemia) plasma glucose concentration. The disease is reportedly the leading cause of adult blindness, end-stage renal failure,

retinopathy, neuropathy, and lower-limb amputations [1]. Diabetes patients are also 2-4 times more likely to develop medical conditions such as heart disease or stroke. Due to the chronic nature and the severity of the complications related to the ailment, diabetes exerts a heavy financial burden on the society. The American Diabetes Association has projected that the annual medical expenditure for diabetes in the United States alone will reach a substantial sum of $\$192$ billion by 2020 [2]. Many of the diabetes related medical complications, however, can be prevented through the tight control of the diabetic blood glucose levels [3, 4].

The current standard treatment procedure of diabetes primarily involves insulin medication coupled with strict dietary control. The insulin hormone is administered through discrete insulin injections, or to a lesser extent, through continuous insulin delivery via an insulin pump. Discrete insulin injections are not therapeutically ideal for the treatment of diabetes since the regulation of the insulin hormone is an open-loop process. Continuous insulin infusion through a programmable insulin pump, on the other hand, offers a potential for a closed-loop glucose regulatory paradigm due to the controllable insulin infusion rate [5]. Many automated glucose regulatory techniques have been proposed, investigated and reported in the literature over the years [6–10]. All such proposed methods employed some forms of models of the human glucose-insulin metabolic process in their control regimes.

Fundamental models [11–13] are constructed by mathematically describing the known physiological glucose metabolic system behaviors such as the underlying glucose and insulin kinetics and transport dynamics in the human body. Due to the use of static mathematical equations, the fundamental modeling approach is inadequate when addressing the issue of patient specificity. The empirical approach, on the other hand, attempts to capture the human glucose metabolic behaviors from the observed input-output clinical data [14]. Based on a predetermined model structure, a set of empirical parameters is subsequently determined for the diabetic patient via data-fitting. The major drawback of the empirical approach stems from the data collection process, where the patients are often subjected to a clinical test environment that introduces artificial conditions such as fixed meal times, a carefully controlled dietary plan and limited exercise. Hence, the resultant glucose metabolic models may not accurately reflect real-life conditions.

Compartmental modeling [10, 15, 16] combines the empirical and fundamental modeling techniques. Such models are derived by compartmentalizing the various physiological components involved in the human metabolic process and subsequently describing each component using fundamentally derived mathematical equations. However, patient-specific parameters are obtained empirically via data fitting. Despite being the most popular approach, some of the endocrine processes affecting glucose metabolism are still not yet fully understood at present and therefore inhibits the effectiveness of the compartmental modeling technique. In particular, the challenge of quantifying the amount and effect of unknown meal disturbances remains a major limitation of the current models of the glucose metabolic process [17].

The fundamental objective of the closed-loop glucose regulatory systems is to artificially re-create (via variable insulin delivery) the healthy insulin profiles (i.e. normal secretion patterns) in a diabetic patient so as to regulate the diabetic blood glucose level within the homeostatic range [18]. Therefore, the performances of these systems to manage diabetes correlate to the accuracy of the models in describing the actual dynamics of the glucose-insulin metabolic process [17]. It has been well established that the human glucose metabolic process is not merely a function of the carbohydrate ingestion, insulin level, and the amount of exercise, but it is also affected by level of stress and other hormonal factors [19–21]. Hence, there is a considerable day-to-day variability in the glucose dynamics of an individual patient as well as across different patients. The primary challenge in the realization of an effective closed-loop regulatory system (also referred to as an artificial pancreas) is therefore the development of a control algorithm that is able to regulate the blood glucose level under a wide range of patient state scenarios [17].

With respect to this notion, there are two major issues that render existing regulatory approaches inadequate. Firstly, the majority of the current closed-loop glucose regulatory systems employ static mathematical or state-space models of the human glucose metabolic process (i.e. compartmentalized physiological modeling) to compute the amount of insulin required by a diabetic patient. These models often require manual tuning to cater for the metabolic biodiversity of the diabetic patients, as well as the intra and inter-day variability in the glucose metabolic rates of each specific patient [12, 22, 23]. Secondly, many of the proposed metabolic models assumed some sort of meal models that require patients to specify the expected time and amount of carbohidrate intake. This enforces strict patient compliance for the resultant closed-loop regulatory systems to function properly. Even then, the therapeutic effects of these pseudo closed-loop systems remained poor and are too rigid and inflexible to be widely employed for diabetes treatment.

In this paper, we propose a novel approach to the synthesize the normal insulin secretion patterns in a diabetic patient. The Pseudo Self-Evolving Cerebellar Model Articulation Controller (PSECMAC) network [24] is employed as an intelligent *insulin schedule* that functionally models the biological process of normal pancreatic insulin secretion in response to serum glucose fluctuations due to food ingestion. The term *insulin schedule* refers to the therapeutic regimens that control the administration of insulin to a diabetic patient based on the observed glucose profile so as to mimic the normal insulin secretion patterns. PSECMAC is an associative learning memory model whose structure and computational principles are inspired by the neurophysiological properties of the human cerebellum that is responsible for human motor control [25–27]. Through PSECMAC, the superior computing capacity of the human cerebellum is harnessed to model the complex and hihgly non-linear glucose-insulin interactions in the human metabolic process.

The proposed PSECMAC intelligent insulin schedule is subsequently employed in a closed-loop glucose regulation system to determine the insulin dosage required by a group of diabetic patients. Our proposed ap-

proach has two distinct advantages. Firstly, the PSECMAC insulin schedule only needs to capture the dynamics of the healthy insulin secretion profile from the observed glucose dynamics and thus eliminating the need to explicitly model and quantify every minute aspect of the human glucose metabolic process, which would otherwise be difficult if not impossible to measure (i.e food intake, stress level, etc). Secondly, the PSECMAC insulin schedule can be easily adapted and customized to address the metabolic biodiversity of the diabetic patients in a diverse population. This paper demonstrates how the proposed PSECMAC intelligent insulin schedule can be applied to regulate the blood glucose level of a diabetic patient under various subject state scenarios.

The rest of this paper is organized as follows. Section 2 briefly describes the PSECMAC network architecture and Section 3 presents the proposed PSECMAC intelligent insulin schedule. In Section 4, the robustness of the PSECMAC insulin schedule against the intra- and inter-day variabilities of the human glucose metabolic process is evaluated. Subsequently, Section 5 demonstrates the use of the proposed PSECMAC intelligent insulin schedule for the management of Type-1 diabetes. Finally, Section 6 concludes this paper.

## 2 The PSECMAC network

The PSECMAC network [24] is a computational model of the human cerebellum. The cerebellum constitutes a vital part of the human brain system that mediates motor movement control and a number of sub-conscious cognitive functions [25, 28]. It functions primarily as a motor movement calibrator [29] and possesses the capability to model highly complex and nonlinear physical dynamics to facilitate the precise and rapid executions of dexterous movements and fluid motor reflexes [30]. PSECMAC was developed to emulate the rapid and nonlinear function learning capability of the cerebellum. Such a computational model has diverse use in applications such as autonomous control [31] and pattern recognition [24, 32, 33] where there are generally no precise mathematical descriptions of the problems characteristics and the inherent process behavior can only be inferred from measurable physical observations.

As a functional computational model of the human cerebellum, PSECMAC manifests as a multi-dimensional multi-resolution associative memory network and employs an error-correction scheme to drive the network learning and knowledge construction process. Figure 1 depicts the structure of a two-input PSECMAC network. The PSECMAC network structure consists of a single layer of computing (memory) cells that are nonlinearly allocated to cover the entire input-output (I/O) mapping space. Each input to the network corresponds to a dimension in the multi-dimensional PSECMAC memory array. The operation of the PSECMAC network is characterized by the multi-resolution table look-up access of its memory cells that facilitates an effective localized generalization and improved modeling accuracy of the network.

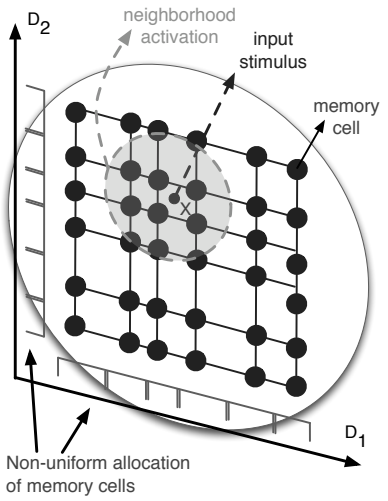


Figure 1: The network structure for a two-input PSECMAC

PSECMAC employs a two-phased learning process, namely: structural learning and parameter tuning. The objective of the structural learning phase is to create the PSECMAC model's associative structure by computing the quantization decision functions for each input dimension. Subsequently, the input to output associative information of the training data samples are learnt by adapting the memory contents of the PSECMAC model in the parameter tuning phase. The detailed description on the PSECMAC network have been repoted in [24].

In summary, the PSECMAC network possesses an effective localized learning capability that enables it to efficiently capture and model complex and dynamic information from the training dataset. In this work, we exploit these computational strengths of PSECMAC to model the biological process of healthy pancreatic insulin secretion and to replicate such insulin release patterns in a diabetic patient.

# 3 The PSECMAC Intelligent Insulin Schedule (Model)

The work presented in this paper is based on the hypothesis that the rate of pancreatic insulin secretion in a healthy person is functionally proportional to the serum insulin concentration measured from time to time. This assumption is adopted because it is currently not technically possible to directly measure the rate of insulin secretion by the human pancreatic $\beta$-cells [34, 35]. The serum insulin concentration therefore constitutes the closest physically-measurable proxy to the rate of pancreatic insulin secretion in the human body, and is thus employed to identify a baseline insulin profile to derive the required insulin schedule. This hypothesis is motivated by the study of the insulin kinetics in the human metabolic system [36] and empirically supported by previous clinical experiments reported in [34, 37] that have established that the insulin concentrations at peripheral veins/arteries are roughly correlated and proportional to the insulin secretion rate of the pancreatic

$\beta$-cells.

As previously described, the term *insulin schedule* here refers to the therapeutic regimens for the administration of insulin to a diabetic patient based on his/her periodically measured glucose profile to maintain the blood glucose level within the normoglycemia range. To achieve the objective of replicating a healthy insulin response in a diabetic patient, the approach adopted in this work is to construct the intelligent insulin schedule using PSECMAC via the modeling of the healthy serum insulin response to the observed glucose level fluctuations. Therefore, the resultant PSECMAC intelligent insulin schedule is essentially a model of the plasma glucose-insulin interactions in the human metabolic process. This methodology is also aligned with the clinical results on continuous insulin infusion experiments reported in [34], which demonstrated that the response of the plasma insulin concentration in human subjects is proportional to the rate of insulin infusion.

The first step to the modeling of the healthy human insulin response is to determine the subject profile to be employed in the study. This section introduces the subject profile adopted in this study, followed by the detailed description of the proposed PSECMAC insulin schedule (model).

## 3.1 The Subject Profile

Due to the lack of real-life patient data and the logistical difficulties and ethical issues involving the collection of such data, a well-known web-based simulator known as *GlucoSim* [38] is employed to simulate a person subject to generate the blood glucose and insulin data that is needed for the construction of the healthy insulin response model. For this purpose, a human profile for the simulated subject (Subject A) is created and described in Table 1. The simulated person, Subject A, is a typical middle-aged Asian male. His body mass index (BMI) is $23.0$ and within the recommended range for Asian. The GlucoSim simulator [39,40] employs a compartmental modeling technique of the human glucose metabolism process. The mathematical models used in GlucoSim to describe the glucose-insulin interactions in both the healthy and diabetic subjects are based on the work of [36] and [10] respectively. The inputs to the GlucoSim simulator for the healthy person model are time and carbohydrate content of the meals taken by the person, the body weight as well as the duration for which the simulation is to be performed.

Based on the profile of Subject A, his recommended daily allowance (RDA) of carbohydrate intake from meals is computed using an applet from the website of the Health Promotion Board of Singapore [41]. According to his sex, age, weight and lifestyle, the recommended daily carbohydrate intake for Subject A is approximately $346.9$g per day. Figure 2 illustrates a sample output from GlucoSim for Subject A based on four meal intakes (i.e. breakfast, lunch, afternoon snack and dinner) that conform to his RDA. This output consists of six elements: blood glucose, blood insulin, intestinal glucose absorption rate, stomach glucose, total glucose

Table 1: The profile of the simulated healthy Subject A

| **Attribute Name** | **Attribute Value** |
|---|---|
| Sex | Male |
| Age | 40 years old |
| Race | Asian |
| Weight | 67 kg (147.71 lbs) |
| Height | 1.70 m (5 ft 7 in) |
| BMI | 23 (Recommended for Asian) |
| Lifestyle | Typical office worker with moderate physical activities such as walking briskly, leisure cycling and swimming. |

uptake rate and liver glucose production rate of Subject A respectively over a simulated time period of 24 hours. The peaks in the stomach glucose subplot of Figure 2 coincide with the timings of the assumed daily four meals (i.e. breakfast, lunch, afternoon snack and dinner) while those peaks in the intestinal glucose absorption rate subplot reflect a delay effect (response) of food intake on the blood glucose level of Subject A. The subplots of blood glucose and blood insulin illustrate the insulin-glucose regulatory mechanism in a healthy person such as Subject A and depict the dynamics of the metabolic process when subjected to disturbances such as food intakes.

Subsequently, *four* types of dietary profiles are defined to simulate the variations in the dietary habit of a human subject. These dietary profile are denoted as *normal*, *under*, *over*, and *irregular* diet. They correspond to the normal, under-eating, overeating, and irregular profiles respectively. The normal diet refers to a dietary profile that conforms to the RDA of the carbohydrate intake of the subject. In this study, the carbohydrate intake of a normal diet for Subject A is defined by eq. (1).

$$\text{normal} \quad \in \quad [0.85 \times \text{RDA}, 1.15 \times \text{RDA}] \tag{1}$$

Similarly, the carbohydrate intakes of the under-eating and the overeating profiles are defined by eqs. (2) and (3) respectively.

$$\text{under} \quad \in \quad [0.425 \times \text{RDA}, 0.575 \times \text{RDA}] \tag{2}$$

$$\text{over} \quad \in \quad [1.275 \times \text{RDA}, 1.725 \times \text{RDA}] \tag{3}$$

The normal, under and over diet profiles are each characterized by *three* regular meals (i.e. breakfast, lunch and dinner) and *one* afternoon snack. The number of meals in the irregular profile, on the other hand, varies between *two* to *six* meals a day, with the carbohydrate intake defined by eq. (4).

$$\text{irregular} \quad \in \quad [0.5, 2.0] \times \text{normal} \tag{4}$$

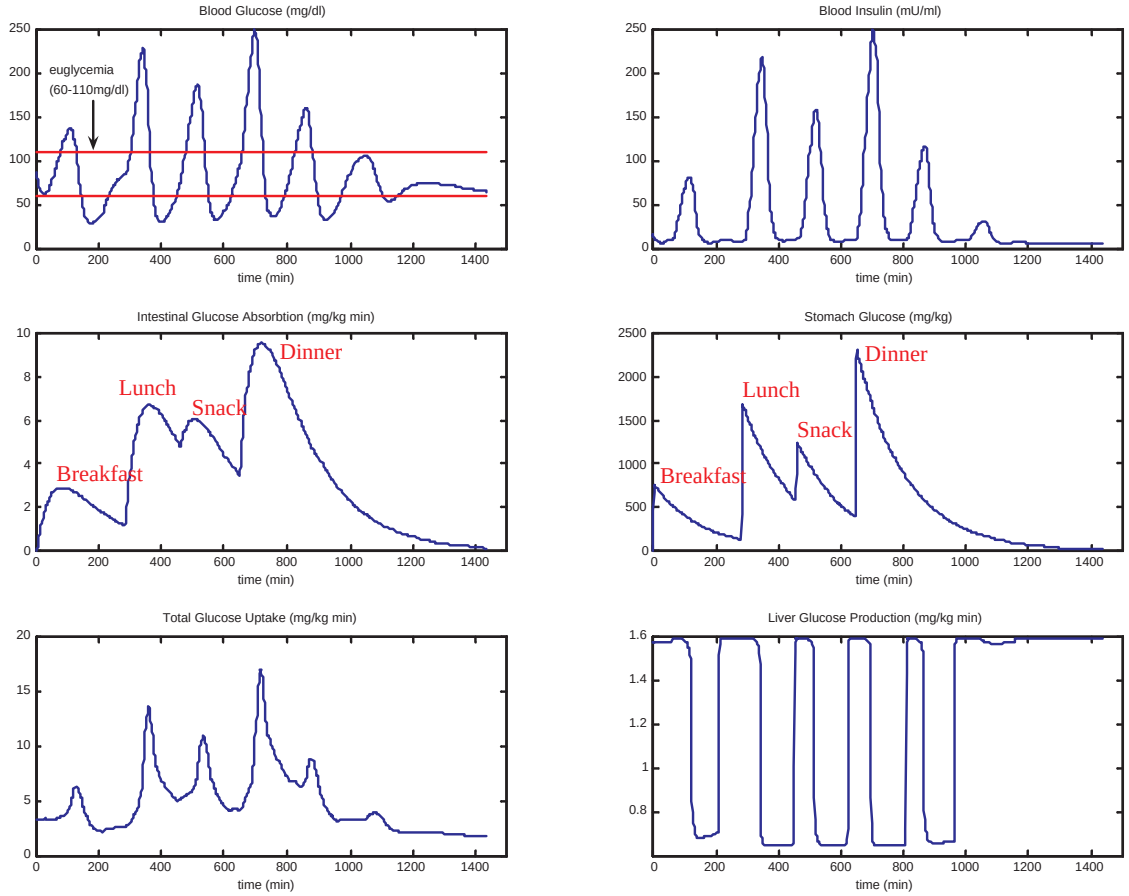


Figure 2: Sample glucose metabolism data output from the GlucoSim simulator

Likewise, the meal timings of the irregular profile are randomized within the day.

In addition, the carbohydrate contents and the timings of the daily meals for each of the normal, under and over diets are not fixed and are varied from day-to-day during the data collection phase. To account for the inter and intra-day variability of the meal contents and the eating habits of Subject A, the computation listed in Table 2 were performed to generate different sets of inputs for each day of the simulated period. These inputs are subsequently used with the GlucoSim simulator to generate the glucose and insulin data.

## 3.2 PSECMAC Modeling of the Healthy Metabolic Insulin Response

In this section, the PSECMAC associative learning memory model is employed to capture the plasma insulin response of Subject A to food ingestion based on the current and past plasma glucose information. The GlucoSim simulator is employed to generate a total of eight days of glucose and insulin data based on the profile of Subject A and his normal dietary habit. The collected metabolic data is subsequently partitioned into two groups: the first 4-days data is used for training the PSECMAC insulin response model, while the remaining

Table 2: Computations for the generation of GlucoSim input parameters for the normal, under and over dietary profiles. (Note: 8 sets of input parameters are generated for each meal profile. U(x,y): a uniformly distributed random number between x and y inclusively; and N($\mu$,$\sigma$): a normally distributed random number with mean $\mu$ and standard deviation $\sigma$.)

| **GlucoSim Input** | **Value** | **Remarks** |
|---|---|---|
| Meal Timings | | Only four meals* per day and meal timings are typical of an office worker |
| Breakfast Time | U(0700hrs,0900$hrs$) | Meal timings are uniformly randomized within their specific ranges |
| Lunch Time | U(1130hrs,1200$hrs$) | |
| Afternoon Snack Time | U(1500hrs,1600$hrs$) | |
| Dinner Time | U(1830hrs,2030$hrs$) | |
| **Total Carbohydrate Intake Per Day** | | TotalCarb = 350g + N($\mu$=0g,$\sigma$=50g) (RDA for Subject A is approx. 350g) |
| Breakfast Carbohydrate | U(12%,18%) $\times$ TotalCarb | Carbohydrate percentages are uniformly randomized within their specific ranges and normalized so that total sum is 100% |
| Lunch Carbohydrate | U(25%,35%) $\times$ TotalCarb | |
| Afternoon Snack Carbohydrate | U(13%,19%) $\times$ TotalCarb | |
| Dinner Carbohydrate | U(35%,45%) $\times$ TotalCarb | |

*It is assumed that Subject A does not take morning and evening snacks. Hence the morning and evening snack timings are kept constant at 1000 and 2200 hours during input to the simulator, and their respective carbohydrate contents are preset to 0g.

4-days data is used for the evaluation of the trained model. A sampling interval of 5 minutes is adopted to discretize the measurements of the blood glucose and insulin concentrations. Let $I_{\text{x}}^{H(P)}$ denotes the insulin profile of the healthy subject P under the dietary profile x $\in \{\text{normal}, \text{under}, \text{over}, \text{irregular}\}$. The insulin relationship to be modelled by the PSECMAC network is formalized as eq. (5) where $\hat{I}_{\text{normal}}^{H(A)}(t+1)$ is the predicted blood insulin concentration at time $t+1$; $\left\{Z_{\text{normal}}^{H(A)}(t)\right\}$ denotes the information set that characterizes the glucose metabolic process of the healthy Subject A due to a normal diet at time $t$; and $\mathfrak{F}(\cdot)$ is a nonlinear function that implements the insulin model mapping from the input metabolic variables $\left\{Z_{\text{normal}}^{H(A)}(t)\right\}$ to the desired output, that is, the blood insulin concentration at the next sampling instance $I_{\text{normal}}^{H(A)}(t+1)$.

$$\hat{I}_{\text{normal}}^{H(A)}(t+1) \quad = \quad \mathfrak{F}_{\text{normal}}^{H(A)}\left(\left\{Z_{\text{normal}}^{H(A)}(t)\right\}\right) \tag{5}$$

Based on the collected blood glucose data, a total of 18 variables (consisting of the current and past blood glucose measurements and its derivatives) are extracted as inputs to model the healthy insulin profile of Subject A. Subsequently, a novel feature selection algorithm named Monte Carlo Evaluative Selection (MCES) [42] is employed to identify the prominent features that best characterize the insulin response of a healthy person. That is, given by eq. (6), for the normal diet, where $\mathfrak{R} = \text{MCES}$ denotes the MCES feature selection process. The reduced set of inputs/features for the normal diet is subsequently denoted by eq (7).

$$\hat{I}_{\text{normal}}^{H(A)}(t+1) \quad = \quad \mathfrak{F}_{\text{normal}}^{H(A)}\left(\mathfrak{R}\left(\left\{Z_{\text{normal}}^{H(A)}(t)\right\}\right)\right) \tag{6}$$

$$\left\{z^{H(A)}_{\text{MCES, normal}}(t)\right\} \quad = \quad \mathfrak{R}\left(\left\{Z^{H(A)}_{\text{normal}}(t)\right\}\right) \tag{7}$$

The MCES method has the advantages of (1) low computational cost; (2) the ability to identify both *correlated* and *irrelevant* features based on weight ranking; (3) being applicable to both classification and regression tasks; and (4) is independent of the underlying induction algorithm used to perform the feature selection process.

The MCES algorithm is executed independently for 50 times, where in each run, 50 iterations on the training set (first 4-days of metabolic data) is performed. This results in a total of 2500 iterations of the training set for the MCES algorithm and the feature ranking results from these executions are aggregated to determine the relevant features for the insulin modeling task. The top four features, namely: the current glucose level ($G(t)$), the 4-point exponential moving average (EMA) of the glucose level ($G_{\text{MA}_M}(t)$), the delta change in the glucose level over the last 5 minutes ($dG(t)$), and the 2-point EMA of the glucose level ($G_{\text{MA}_S}(t)$) are selected as the glucose indicators/inputs to the PSECMAC insulin response model. The computational objective of the PSECMAC insulin response model is subsequently formalized as eq. (8) where $I^{H(A)}_{\text{normal}}(t+1)$ is the actual measured blood insulin level at time $t+1$.

$$\begin{aligned}&\left\|I^{H(A)}_{\text{normal}}(t+1) - \hat{I}^{H(A)}_{\text{normal}}(t+1)\right\|_{\text{minimize}} \\ &\qquad = \quad \left\|I^{H(A)}_{\text{normal}}(t+1) - \mathfrak{F}^{H(A)}_{\text{normal}}\left(\left\{z^{H(A)}_{\text{MCES, normal}}(t)\right\}\right)\right\|_{\text{minimize}}\end{aligned} \tag{8}$$

A PSECMAC network with a memory size of $8$ cells per dimension is constructed to model the insulin profile of the healthy subject as shown in eq. (6). A neighborhood size (N) of $0.1$ and a Gaussian width constant ($\gamma$) of 0.3 have been empirically determined to give the optimal modeling performance. As benchmarks, the insulin modeling task is also performed using various well-established empirical models. The benchmarking models studied in this work are the classical cerebellar computational model of the Cerebellar Model Articulation Controller (CMAC) network [43, 44]; two other cerebellar-based architectures, namely: (1) the HCAQ-CMAC network [31] and (2) the Fuzzy CMAC with Yager Inference Scheme (FCMAC-Yager) [45]; a well-established neuro-fuzzy system termed the Generic Self-Organizing Fuzzy Neural Network (GenSoFNN-CRI) [46]; as well as the classical machine learning models of the Radial Basis Function (RBF) network [47] and the Multi-Layered Perceptron (MLP). The parameters for the FCMAC-Yager and the GenSoFNN-CRI systems have all been empirically optimized for best performances. There are two network structures of the MLP, each having one and two hidden layers respectively. These have also been empirically determined. The RBF network is initialized to contain 50 hidden layer nodes. In addition, the size of the CMAC and the HCAQ-CMAC networks has been defined as 8 cells per dimension for a fair comparison with the proposed PSECMAC insulin response model.

Table 3: Simulation results for the various insulin response models

| | **Recall** | | | **Generalization** | | | | | |
|---|---|---|---|---|---|---|---|---|---|
| **Network** | **RMSE** | **PC** | **$PI_1$** | **RMSE** | **PC** | **$PI_1$** | **MAE** | **MSE** | **$PI_2$** |
| **PSECMAC** | **6.3011** | **0.9918** | **13.58** | **4.0737** | **0.9948** | **19.61** | **2.1187** | **16.595** | **5.32** |
| CMAC | 4.4990 | 0.9958 | 18.11 | 6.6692 | 0.9880 | 12.88 | 4.6351 | 44.478 | 7.89 |
| HCAQ-CMAC | 4.3494 | 0.9961 | 18.62 | 5.6357 | 0.9905 | 14.92 | 3.4779 | 31.761 | 7.09 |
| FCMAC-Yager | 6.7013 | 0.9929 | 12.89 | 6.8474 | 0.9899 | 12.61 | 6.0575 | 46.887 | 6.64 |
| GenSoFNN-CRI | 6.6710 | 0.9944 | 12.96 | 5.8942 | 0.9953 | 14.44 | 4.7014 | 34.742 | 6.09 |
| MLP (4-120-1) | 26.337 | 0.8861 | 3.24 | 24.291 | 0.8552 | 3.38 | 20.666 | 590.05 | 27.23 |
| MLP (4-20-4-1) | 23.450 | 0.8908 | 3.64 | 21.757 | 0.8607 | 3.78 | 18.637 | 473.37 | 24.11 |
| RBF | 6.4141 | 0.9915 | 13.37 | 5.3977 | 0.9906 | 15.48 | 3.4419 | 29.135 | 6.56 |

Table 3 lists the *recall* (in-sample testing) and the *generalization* (out-of-sample testing) performances of the various benchmarked insulin models. *RMSE* denotes the root-mean-squared-error between the set of computed and expected insulin levels; and *PC* is the Pearson correlation coefficient, a statistical measure reflecting the goodness-of-fit between the computed and expected insulin dynamics. A *performance index* ($PI_1$) measure is used to combine the RMSE and the PC values of the benchmarked networks as described in eq. (9).

$$\mathrm{PI}_1 \quad = \quad \frac{\mathrm{PC}}{1+\mathrm{RMSE}} \times 100, \qquad \mathrm{PI}_1 \in [-100, 100] \tag{9}$$

such that a higher $PI_1$ value corresponds to a better overall prediction performance of the insulin model. In addition, the generalization results are also reported in terms of the *mean-absolute-error* (MAE) and the *mean-squared-error* (MSE) values of the computed insulin response. The MSE measure magnifies the larger errors between the computed and the actual insulin concentrations; hence the impact of these errors is pronounced for this measure. Together with the MAE value, this would allow one to discern amongst the insulin models that give consistent but minute errors from the insulin models that provide highly accurate predictions at most of the sampled points but with occasional large errors. The MSE and MAE measures are subsequently combined as shown in eq. (10), such that a lower $PI_2$ value implies a more consistent prediction performance of the model.

$$\mathrm{PI}_2 \quad = \quad \frac{\mathrm{MSE}}{1+\mathrm{MAE}}, \qquad \mathrm{PI}_2 \in [0, \infty] \tag{10}$$

As shown in Table 3, the PSECMAC insulin response model achieved the best generalization performances among all the benchmarked models. The generalization evaluation of the PSECMAC model results in the highest $PI_1$ value and the lowest $PI_2$ value, which demonstrate the accuracy and consistency in its predicted insulin responses. The generalization results of the PSECMAC model outperformed those of the benchmarked cerebellar-based architectures (i.e. the CMAC, HCAQ-CMAC and FCMAC-Yager networks), thereby demonstrating the effectiveness of the PSECMAC network as a cerebellar-based insulin response model. While the

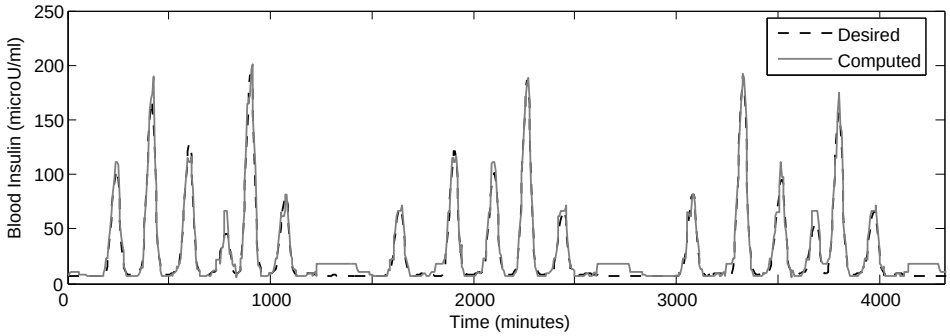


(a) CMAC Insulin Model

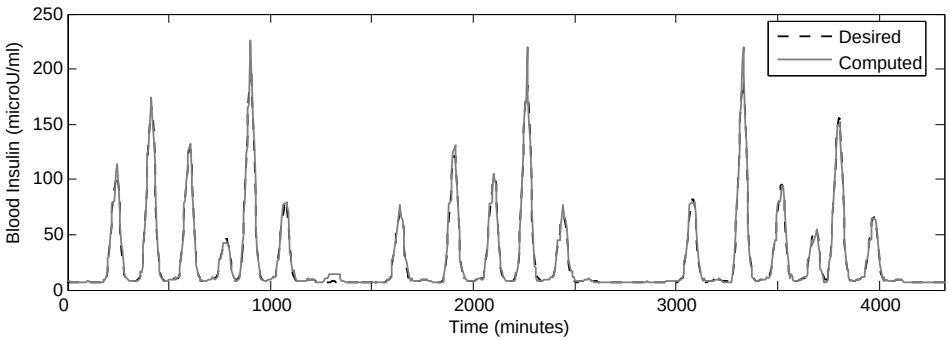


(b) PSECMAC Insulin Model

Figure 3: 3-days generalization performances of the CMAC and PSECMAC networks in modeling the insulin profile of a healthy person

uniform quantization process of the CMAC network results in a lower accuracy of the computed output, the non-uniform quantization process of the HCAQ-CMAC network employs a hierarchical clustering technique that groups together neighboring regions of inputs having similar outputs. Although this approach is highly effective in optimizing the generalization ability of the HCAQ-CMAC network, it may result in a reduced output accuracy as in the case of the insulin prediction task. The FCMAC-Yager network, on the other hand, is a Mamdani fuzzy rule-based system that adopts trapezoidal-shaped fuzzy sets as membership functions. This often leads to a low output accuracy due to the coarse granularity of the membership functions.

The recall performances of the PSECMAC insulin response model, however, are slightly inferior to those of its uniformly-quantized CMAC counterpart. This is because the static structure of the basic CMAC network results in a model that is optimized for the training set. The adaptive memory quantization mechanism of the PSECMAC network, on the other hand, is better equipped towards obtaining an efficient characterization of the complex and intertwined glucose–insulin relationships. This enables the PSECMAC network to achieve an improved generalization result despite poorer recall performances as demonstrated by the simulation results on the insulin prediction task. In contrast, a significant performance degradation is observed for the CMAC insulin response model as the emphasis is shifted from the recall to the generalization evaluation.

In addition, the PSECMAC insulin response model achieved a $26.7\%$ higher $((19.61 - 15.48)/15.48)$ $\text{PI}_1$ value and a $18.9\%$ $((6.56-5.32)/5.32)$ lower $\text{PI}_2$ value over the best performing benchmarked non-cerebellar-based model (i.e. RBF) for the generalization evaluation. The PSECMAC network has comprehensively outperformed the benchmarked GenSoFNN-CRI neuro-fuzzy system and the classical machine learning technique-based (i.e. MLP, RBF) insulin models. The simulation results outlined in Table 3 have also demonstrated the inability of MLP in capturing the underlying relationships between the glucose indicators and the insulin responses. Both the 3-layers and 4-layers MLPs reported the poorest recall and generalization performances amongst the benchmarked systems. Figure 3 depicts a 3-days snapshot of the generalization performances of the CMAC and PSECMAC insulin response models. Simulation results shown in Figure 3 and Table 3 have sufficiently demonstrated the highly encouraging accuracy of the PSECMAC insulin response model in predicting the correct insulin response based on the selected glucose indicators.

# 4 PSECMAC Modeling of the Healthy Insulin Response under Varying Dietary Profiles

As discussed in the Introduction, it is highly desirable to have a closed-loop glucose-insulin regulatory system that is able to address the intra- and inter-day variability observed in the human glucose metabolic process. In this section, the robustness of the proposed PSECMAC insulin response model against the intra-day variability in the metabolic process of a healthy person is investigated. The objective of the study is to evaluate how the insulin response model $\mathfrak{F}^{H(A)}_{\text{normal}}$ (see eq. (6)) responds to the different dietary profiles of Subject A. For example, the computed insulin response when Subject A *overeats* based on the insulin model $\mathfrak{F}^{H(A)}_{\text{normal}}$ is defined as eq. (11) where $\left\{z^{H(A)}_{\text{MCES,over}}(t)\right\}$ denotes the set of glucose indicators extracted from the dietary data of Subject A when he overeats. Note that the set of glucose indicators fed as inputs to the PSECMAC insulin response model is the same for all the dietary profiles evaluated in this section. That is, the inputs are the salient glucose variables identified by the MCES feature selection process in Section 3.2. Hence, the purpose of the computational experiments performed in this section is essentially to ascertain whether the insulin response $\hat{I}^{H(A)}_{\text{normal(x)}}(t+1)$ is a good approximator of $I^{H(A)}_{\text{x}}(t+1)$, where $\text{x} \in \{\text{under}, \text{over}, \text{irregular}\}$ denotes the different dietary profiles, $\hat{I}^{H(A)}_{\text{normal(x)}}(t+1)$ is the insulin response computed with the insulin response model $\mathfrak{F}^{H(A)}_{\text{normal}}$ that is constructed from the dietary data of Subject A according to his normal diet, and $I^{H(A)}_{\text{x}}(t+1)$ is the actual insulin response as observed from the metabolic data of Subject A.

$$\hat{I}^{H(A)}_{\text{normal(over)}}(t+1) \quad = \quad \mathfrak{F}^{H(A)}_{\text{normal}}\left(\left\{z^{H(A)}_{\text{MCES,over}}(t)\right\}\right) \tag{11}$$

Table 4: Simulation results of the PSECMAC and CMAC insulin response models for the various dietary profiles

| **Network** | **Dietary Profile** | **RMSE** | **PC** | **$PI_1$** | **MAE** | **MSE** | **$PI_2$** |
|---|---|---|---|---|---|---|---|
| PSECMAC | Normal | 4.0737 | 0.9948 | 19.61 | 2.1187 | 16.595 | 5.32 |
| | Undereat | 3.3064 | 0.9930 | 23.06 | 1.6454 | 10.932 | 4.13 |
| | Overeat | 17.668 | 0.9765 | 5.23 | 5.8056 | 312.16 | 45.87 |
| | Irregular | 34.769 | 0.9259 | 2.59 | 7.4270 | 1208.9 | 143.5 |
| CMAC | Normal | 6.6692 | 0.9880 | 12.88 | 4.6351 | 44.478 | 7.89 |
| | Undereat | 5.8997 | 0.9818 | 14.23 | 3.8684 | 34.806 | 7.15 |
| | Overeat | 24.680 | 0.9433 | 3.67 | 7.9923 | 609.10 | 67.74 |
| | Irregular | 40.319 | 0.8797 | 2.13 | 9.4144 | 1625.6 | 156.1 |

Table 5: Performance comparisons between the PSECMAC and CMAC insulin response models for the various dietary profiles

| **Dietary** | **$PI_1$** | | | **$PI_2$** | | |
|---|---|---|---|---|---|---|
| **Profile** | **PSECMAC** | **CMAC** | **% Gain** | **PSECMAC** | **CMAC** | **% Gain** |
| Normal | 19.61 | 12.88 | 52.25 | 5.32 | 7.89 | 32.57 |
| Undereat | 23.06 | 14.23 | 62.05 | 4.13 | 7.15 | 42.24 |
| Overeat | 5.23 | 3.67 | 42.51 | 45.87 | 67.74 | 32.29 |
| Irregular | 2.59 | 2.13 | 21.60 | 143.5 | 156.1 | 8.07 |
| **Average** | | | **$44.60\%$** | | | **$28.79\%$** |

For the simulations, a set of 4 days of glucose and insulin data is generated for each of the dietary profiles using GlucoSim. The PSECMAC insulin response model trained with the data extracted from the normal dietary profile (as in Section 3.2) is then applied to respectively predict the healthy insulin responses for the different dietary profiles (i.e. under, over and irregular eating). Table 6 tabulates the performances of the PSECMAC model in predicting the insulin responses for the various dietary profiles. The RMSE, PC, $PI_1$, MAE, MSE, and $PI_2$ values are employed as the performance measures of the PSECMAC insulin response model. In this paper, the CMAC network is employed as the key benchmark architecture to assess the performance of the trained PSECMAC insulin model. This is because beside being the predecessor to PSECMAC, the CMAC network is also widely-used in control applications [48,49] and therefore constitutes a highly viable model for insulin regulation in a closed loop setup. Table 4 oulines the insulin prediction performances of both the CMAC and the PSECMAC insulin models for the various dietary profiles. Table 5 subsequently lists the detailed performance comparisons between the PSECMAC and CMAC insulin response models for all the dietary profiles.

From the results tabulated in Tables 4 and 5, one can observe that the PSECMAC insulin response model has comprehensively outperformed the benchmarked CMAC insulin response model for all the evaluated dietary profiles. The PSECMAC insulin response model yielded, on average, a $44\%$ increment in $PI_1$ and a $29\%$ decrement in $PI_2$ over the CMAC insulin response model. The highest performance gains of the PSECMAC over the CMAC insulin response model were noted for the undereat diet, with gains of $62\%$ and $42.2\%$ in

the $PI_1$ and $PI_2$ values respectively. These gains are even higher than those for the normal diet (i.e. $PI_1$ gain of $52.3\%$ and $PI_2$ gain of $32.6\%$), for which the PSECMAC and CMAC insulin response models have been specifically trained. However, Table 5 also shows that the performance gains of the PSECMAC over the CMAC insulin response model are lower for the overeat and irregular dietary profiles. This is due to the substantial decrease in the $PI_1$ and $PI_2$ values achieved by the PSECMAC insulin response model for the overeat and irregular diets despite its superiority over the benchmarked CMAC insulin response model. These observations are analyzed as follows.

The undereat dietary profile provides an evaluation on the sensitivity of the trained insulin models to the smaller fluctuations in the blood glucose concentration resulting from the reduced carbohydrate intakes. Figure 4 depicts the 3-days computed insulin responses of the CMAC and PSECMAC insulin response models for the undereat diet. As shown in Figure 4, both the CMAC and PSECMAC insulin response models were able to achieve a rather precise fit to the actual (desired) insulin response of Subject A. This is because the undereat diet is metabolically an attenuation of the normal dietary profile (refer to eq. (2)). Therefore, the training derived from the normal dietary profile is functionally adequate to *prime* the insulin models with the necessary characteristic mappings or domain knowledge to predict the insulin requirements for the undereat diet.

However, the computed insulin responses of the CMAC insulin response model were plagued by offset errors (refer to $B_1$, $B_2$ and $B_3$ of Figure 4(a)) that contribute to its poorer performances. In addition, several overshoots were noted in the computed CMAC insulin responses as highlighted by $A_1$ and $A_2$ in Figure 4(a). These offsets and overshoots in the computed insulin responses may be attributed to the uniform partitioning of the input–output mapping space of the basic CMAC network. The uniform quantization of the CMAC memory space results in a static output resolution throughout the entire CMAC input space, and this often leads to an averaging effect and reduced output precision as manifested in the offsets and overshoots of Figure 4(a). In contrast, the PSECMAC network non-uniformly allocates its memory cells according to the characteristics of the training data, where more memory cells (and hence higher output resolutions) are allocated to the significant regions of the input space. This enables PSECMAC to compute an accurate prediction of the insulin responses of Subject A for the undereat dietary profile (as shown by $P_1$ and $P_2$ in Figure 4(b)).

The overeat and irregular dietary profiles, on the other hand, stimulate the uncertainty associated with the meal consumption habits of Subject A and the inter-day variability of his metabolism process. This sought to investigate the robustness of the PSECMAC and CMAC-based insulin response models under demanding conditions. Similar to the normal and undereat profiles, the overeat diet is characterized by four daily meals. The total daily carbohydrate intake when Subject A overeats, however, is greater than his recommended daily allowance (refer to eq. (3)). Hence, overeating causes the CMAC and PSECMAC insulin response models to be subjected to meal (carbohydrate) intakes that exceed those of the normal diet (from which the models

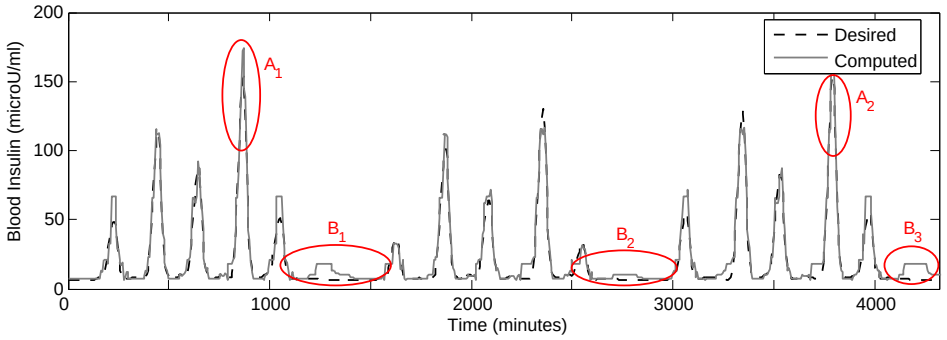


(a) CMAC Insulin Model

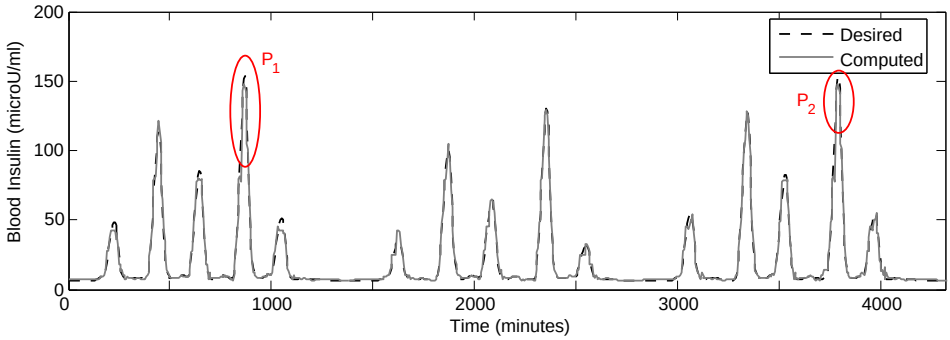


(b) PSECMAC Insulin Model

Figure 4: 3-days generalization performances of the CMAC and PSECMAC network in modeling the insulin profile of Subject A for the undereat diet

have previously been derived). The overeat diet effectively assesses the capacity of the insulin models in responding to the augmented fluctuations and increased levels of the glucose concentrations that are above the range encountered in the normal profile. On the other hand, the irregular dietary profile is defined based on the day-to-day variation in the amount of carbohydrate consumed together with the sporadic number of meals taken by Subject A in a day. As described in Section 3.1, the number of meals for the irregular dietary profile varies between 2 to 6 meals per day while the amount of daily carbohydrate intakes ranges between half to twice of the RDA for Subject A. Therefore, the irregular diet essentially evaluates the performances of the trained PSECMAC and CMAC insulin respose models for a challenging set of circumstances that is characterized by both large (rapid) and small (slow) fluctuations in the measured blood glucose concentrations.

Figures 5 and 6 depict the 3-days generalization results of the CMAC and PSECMAC insulin response models for the overeat and irregular dietary profiles respectively. Based on the two figures, several observations can be made of the generalization performances of the two insulin models. Firstly, although the computed insulin responses of both the CMAC and the PSECMAC insulin response models were able to closely match the actual (desired) insulin responses of the healthy subject within the range of low to moderate insulin values, both insulin models failed to track the occasional high peaks in the healthy insulin profile arising from the large

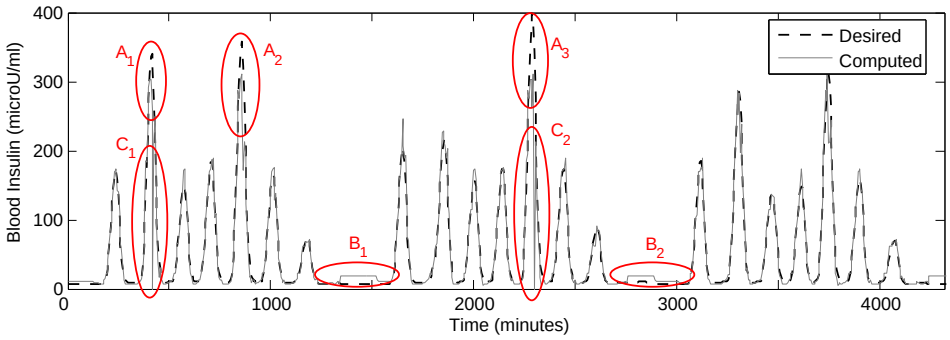


(a) CMAC Insulin Model

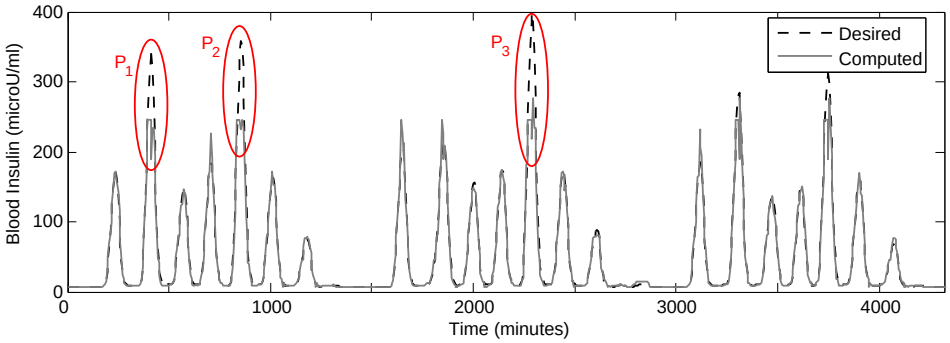


(b) PSECMAC Insulin Model

Figure 5: 3-days generalization performances of the CMAC and PSECMAC network in modeling the insulin profile of Subject A for the overeat dietary profile

amount of carbohydrate intakes associated with overeating. The poor generalization performances of both models for the prominent peaks of the overeat and irregular diets are thus primarily due to the large undershoot errors, as highlighted by $A_1$, $A_2$ and $A_3$ in Figure 5(a), as well as $P_1$, $P_2$ and $P_3$ in Figure 5(b).

These undershoot errors are due to the fact that no prior training has been performed to enable the models to derive the required insulin responses for large-sized meal disturbances, as a large amount of carbohydrate intake results in a surge of the blood glucose levels to a range that is beyond the information that has been extracted from the normal diet. Consequently, as the insulin response of a healthy person is dependent on the circulating blood glucose concentration, a high carbohydrate intake will result in a large undershoot error. This is especially evident in the generalization results for the irregular diet depicted in Figure 6 (see $A_1$ and $A_2$ of Figure 6(a) and $P_1$ and $P_2$ of Figure 6(b)).

Secondly, the lack of model training for the large-sized meal scenarios in the overeat and irregular diets also gives rise to the *empty cells phenomena* that degrades the consistency of the predicted insulin responses of the CMAC insulin response model. The empty cells phenomena in a CMAC-based system occurs whenever the input vector accesses the regions of untrained CMAC memory cells and thus resulting in an undesirable system output. In this example, the effects of the untrained CMAC cells are highlighted as $C_1$ and $C_2$ in Figures 5(a)

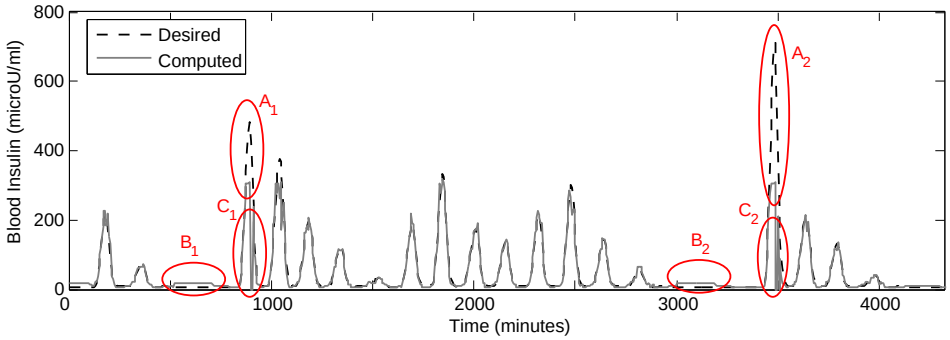


(a) CMAC Insulin Model

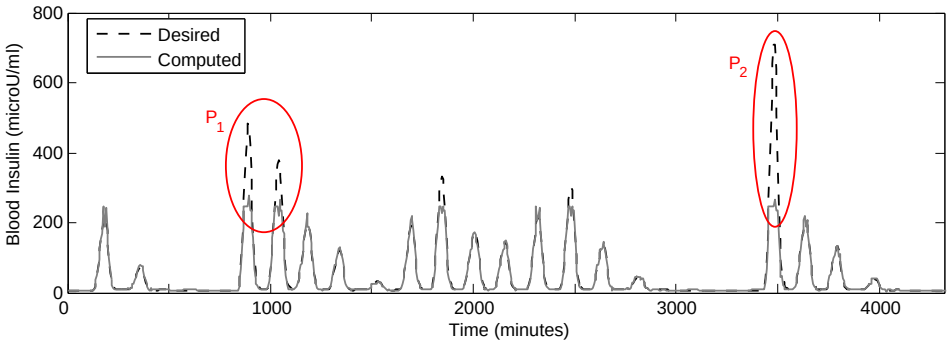


(b) PSECMAC Insulin Model

Figure 6: 3-days generalization performances of the CMAC and PSECMAC network in modeling the insulin profile of Subject A for the irregular dietary profile

and 6(a). On the other hand, the non-uniform memory quantization scheme of the PSECMAC architecture allows the PSECMAC insulin response model to better generalize the characteristics of the glucose–insulin relationships. This enables the PSECMAC insulin response model to compute a reasonable prediction of the insulin response even for an input vector that has not been encountered before. Lastly, similar to the evaluation results observed of the undereat diet, the computed CMAC insulin responses suffer from offset errors that further degrade the performances of the CMAC insulin model (see $B_1$ and $B_2$ of Figures 5(a) and 6(a)).

To complete the assessment of the PSECMAC insulin model, the set of simulations is repeated using the remaining similarly-trained benchmark systems of Section 3.2 and the results are presented in Table 6. From the results tabulated in Table 6, it is evident that the PSECMAC insulin model generally outperformed the benchmark insulin models. Similar to the results of the insulin modeling task of the normal dietary profile presented in Section 3.2, the PSECMAC insulin model comprehensively outperformed the cerebellar-based architectures for all the evaluated dietary profiles. The trained PSECMAC insulin model also achieved superior prediction performances over the benchmarked MLP and GenSoFNN-CRI models. The RBF-based insulin model, however, reported a slight performance improvement over the PSECMAC model for the overeat dietary profile. This minute performance inferiority can be attributed to the effect of insufficient training in the PSECMAC

Table 6: Simulation results of the insulin response models for the various dietary profiles

| **Network** | **Dietary Profile** | **RMSE** | **PC** | **$PI_1$** | **MAE** | **MSE** | **$PI_2$** |
|---|---|---|---|---|---|---|---|
| PSECMAC | Normal | 4.0737 | 0.9948 | 19.61 | 2.1187 | 16.595 | 5.32 |
| | Undereat | 3.3064 | 0.9930 | 23.06 | 1.6454 | 10.932 | 4.13 |
| | Overeat | 17.668 | 0.9765 | 5.23 | 5.8056 | 312.16 | 45.87 |
| | Irregular | 34.769 | 0.9259 | 2.59 | 7.4270 | 1208.9 | 143.5 |
| HCAQ-CMAC | Normal | 5.6357 | 0.9905 | 14.92 | 3.4779 | 31.761 | 7.09 |
| | Undereat | 5.1075 | 0.9842 | 16.11 | 3.0007 | 26.087 | 6.52 |
| | Overeat | 19.567 | 0.9659 | 4.69 | 7.0539 | 382.87 | 47.54 |
| | Irregular | 54.017 | 0.7664 | 1.39 | 10.447 | 2917.8 | 254.9 |
| FCMAC-Yager | Normal | 6.8474 | 0.9899 | 12.61 | 6.0575 | 46.887 | 6.64 |
| | Undereat | 6.7976 | 0.9849 | 12.63 | 6.2401 | 46.207 | 6.38 |
| | Overeat | 40.338 | 0.8398 | 2.03 | 10.914 | 1627.2 | 136.6 |
| | Irregular | 66.382 | 0.6070 | 0.90 | 16.123 | 4406.6 | 257.3 |
| GenSoFNN-CRI | Normal | 5.8942 | 0.9953 | 14.44 | 4.7014 | 34.742 | 6.09 |
| | Undereat | 5.5689 | 0.9932 | 15.12 | 4.6603 | 31.013 | 5.48 |
| | Overeat | 23.328 | 0.9560 | 3.93 | 8.2062 | 544.2 | 59.11 |
| | Irregular | 42.096 | 0.8804 | 2.04 | 10.658 | 1772.1 | 152.0 |
| MLP (4-120-1) | Normal | 24.291 | 0.8552 | 3.38 | 20.666 | 590.05 | 27.23 |
| | Undereat | 21.922 | 0.8165 | 3.56 | 19.526 | 480.6 | 23.4 |
| | Overeat | 34.019 | 0.9083 | 2.59 | 25.246 | 1157.3 | 44.09 |
| | Irregular | 50.236 | 0.9610 | 1.88 | 32.891 | 2523.7 | 74.47 |
| MLP (4-20-4-1) | Normal | 21.757 | 0.8607 | 3.78 | 18.637 | 473.37 | 24.11 |
| | Undereat | 21.269 | 0.8318 | 3.74 | 18.833 | 452.4 | 22.81 |
| | Overeat | 32.699 | 0.9139 | 2.71 | 24.949 | 1069.2 | 41.20 |
| | Irregular | 45.280 | 0.9341 | 2.02 | 28.116 | 2050.3 | 70.42 |
| RBF | Normal | 5.3977 | 0.9906 | 15.48 | 3.4419 | 29.135 | 6.56 |
| | Undereat | 3.9704 | 0.9899 | 19.92 | 2.5791 | 15.764 | 4.40 |
| | Overeat | 14.010 | 0.9838 | 6.55 | 6.5549 | 196.3 | 25.94 |
| | Irregular | 51.525 | 0.7901 | 1.50 | 10.495 | 2654.8 | 230.95 |

network. Due to the PSECMAC localized learning scheme, the training dataset on the normal dietary profile is not sufficient to equip the trained PSECMAC insulin model with an accurate response for the high insulin peaks associated with the overeat diet. This effect is less pronounced in the RBF-based insulin model due to a larger steady state error, as evidenced by the higher MAE value of the RBF-based insulin prediction results for the overeat diet in comparison to that of the PSECMAC model. Nevertheless, the superior performances of the PSECMAC insulin model over its RBF-based counterpart on the normal, undereat and irregular dietary profiles further reinforced the choice of the PSECMAC network for the modeling of the insulin response in a healthy subject.

From the results of the previous computational experiments, one can conclude that the poor performances of the PSECMAC and other benchmarked insulin response models for the overeat and irregular dietary evaluations are predominantly caused by the lack of prior training on large-sized meal disturbances. Therefore, in order to enhance the generalization performances, the trained insulin response models are dynamically tuned to adapt

Table 7: Simulation results of the tuned insulin models for the overeat and irregular dietary profiles

| **Network** | **Dietary Profile** | **RMSE** | **PC** | **$PI_1$** | **MAE** | **MSE** | **$PI_2$** |
|---|---|---|---|---|---|---|---|
| PSECMAC | Overeat | 9.9580 | 0.9922 | 9.05 | 4.8759 | 99.162 | 16.88 |
| | Irregular | 19.089 | 0.9763 | 4.86 | 6.9385 | 364.40 | 45.90 |
| CMAC | Overeat | 22.943 | 0.9512 | 3.97 | 6.8259 | 526.36 | 67.26 |
| | Irregular | 23.846 | 0.9621 | 3.87 | 11.884 | 568.63 | 44.13 |
| GenSoFNN-CRI | Overeat | 11.616 | 0.9918 | 7.86 | 6.1869 | 134.93 | 18.77 |
| | Irregular | 26.473 | 0.96425 | 3.51 | 13.722 | 700.82 | 47.60 |

Table 8: Performance comparisons between the tuned insulin models for the various dietary profiles

| | | **$PI_1$** | | | | |
|---|---|---|---|---|---|---|
| **Dietary Profile** | **Tuning Phase** | **PSECMAC** | **CMAC** | **GenSoFNN-CRI** | **% Gain1** | **% Gain2** |
| Overeat | Before | 5.23 | 3.67 | 3.93 | 42.51% | 33.08% |
| | After | 9.05 | 3.97 | 7.86 | 127.9% | 15.14% |
| | % Improve | 73.04% | 8.17% | 99.49% | | |
| Irregular | Before | 2.59 | 2.13 | 2.04 | 21.60% | 27.94% |
| | After | 4.86 | 3.87 | 3.51 | 25.58% | 38.46% |
| | % Improve | 87.64% | 81.69% | 72.06% | | |
| | | **$PI_2$** | | | | |
| **Dietary Profile** | **Tuning Phase** | **PSECMAC** | **CMAC** | **GenSoFNN-CRI** | **% Gain1** | **% Gain2** |
| Overeat | Before | 45.87 | 67.74 | 59.11 | 32.29% | 22.40% |
| | After | 16.88 | 67.26 | 18.77 | 74.90% | 10.07% |
| | % Improve | 63.20% | 0.71% | 68.25% | | |
| Irregular | Before | 143.5 | 156.1 | 152.0 | 8.07% | 5.59% |
| | After | 45.90 | 44.13 | 47.60 | −4.01% | 3.57% |
| | % Improve | 68.01% | 71.73% | 68.68% | | |

their learnt schedules to the overeat and the irregular dietary profiles. For this purpose, a set of 4-days (new) glucose and insulin data is generated for each of the overeat and irregular diets respectively using the GlucoSim simulator for Subject A. The collected data is subsequently employed to tune the trained insulin response models. In this study, the adaptation process of the PSECMAC insulin model is compared to those of the CMAC and GenSoFNN-CRI models. These two benchmark models are selected because they possess online learning capability that enables the continuous adaptation of the insulin response to a new dietary profile. Tables 7 and 8 list the generalization performances of the tuned insulin response models for the overeat and irregular dietary profiles. The "% Gain1" and "% Gain2" measures denote the percentage gain in the performances of the PSECMAC insulin response model over its CMAC and GenSoFNN-CRI counterparts. The "% Improve" measure, on the other hand, computes the percentage of performance improvement achieved by the tuning process of the respective insulin models. As an illustration, the 3-days predicted insulin responses of the tuned CMAC and PSECMAC insulin response models are depicted in Figures 7 and 8 for the overeat and irregular diets respectively.

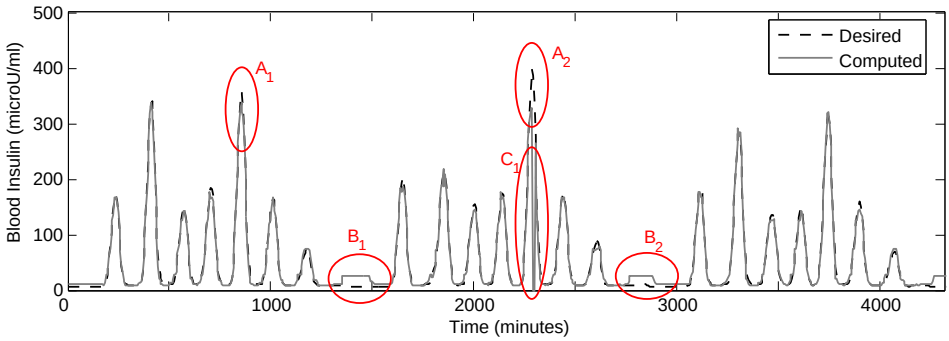


(a) CMAC Insulin Model

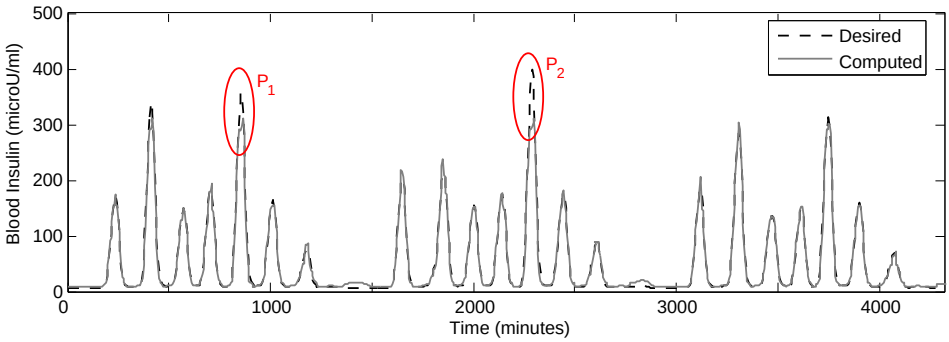


(b) PSECMAC Insulin Model

Figure 7: 3-days generalization performances of the CMAC and PSECMAC networks (after-tuning) in modeling the insulin profile of Subject A for the overeat dietary profile

From the results tabulated in Tables 7 and 8, one can observe that the tuning process leads to substantial improvements in the performances of all the benchmarked insulin response models. In accordance with the earlier hypothesis, the adaptive tuning mechanism enabled both the CMAC and PSECMAC insulin response models to compute more accurate predictions of the insulin responses for the peaks associated with the large carbohydrate intakes present in the overeat and irregular diets. These are highlighted as $A_1$, $A_2$ and $P_1$, $P_2$ of Figures 7 and 8. In addition, the adaptive tuning has also increased the gain in the performance (% Gain) of the PSECMAC insulin response model over its CMAC counterpart for the overeat diet. This is due to the fact that the non-uniform quantization scheme of the PSECMAC network allows for better characterization of the selected glucose variables to insulin responses relationships. As highlighted in $B_1$, $B_2$ and $C_1$ of Figure 7(a), the suboptimal static quantization of the CMAC memory cells has resulted in the offset errors and the occurrence of the empty cell phenomena in the predicted CMAC insulin responses.

However, with respect to Table 7, the generalization performances of the CMAC insulin response model for the irregular dietary profile after the tuning process are comparable to those of the PSECMAC model. As depicted in Figure 8(b), the PSECMAC insulin response model exhibited a considerable undershoot error (highlighted as $P_1$) despite being able to compute fairly accurate predictions of the insulin responses for most

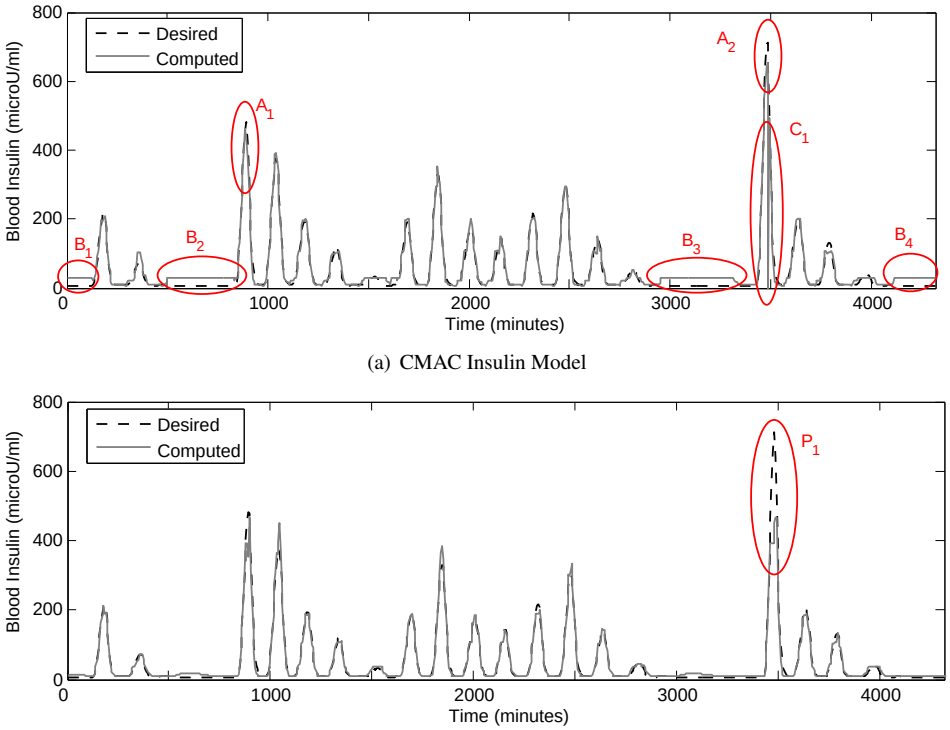


(a) CMAC Insulin Model

(b) PSECMAC Insulin Model

Figure 8: 3-days generalization performances of the CMAC and the PSECMAC networks (after-tuning) in modeling the insulin profile of Subject A for the irregular dietary profile

of the sampled points. This is due to the fact that the extra 4-days of new metabolic data might not be sufficient to capture the comprehensive characteristics of the irregular diet. In contrast to the overeat profile that adopts a constant 4-meals-a-day regime, the irregular dietary profile varies the number of meals taken together with an enlarged range for the daily total carbohydrate intakes. Such irregularities (uncertainties) translate to large permutations of eating patterns (i.e. insulin profile) that cannot be comprehensively characterized by only 4-days of metabolic data. Therefore, it is highly plausible that insufficient training (tuning) accounts for the uncharacteristically large undershoot errors observed in the computed PSECMAC insulin responses. On the other hand, the averaging principle in the output computation process of the CMAC network would likely have assisted in improving the overall performance of the CMAC insulin response model. However, from Figure 8(a), it can be observed that the computed CMAC insulin responses suffer from many offset errors (see $B_1$, $B_2$, $B_3$ and $B_4$) as well as the empty cell phenomena (i.e. $C_1$). Therefore, by comparing the computed insulin responses of the CMAC (Figure 8(a)) and PSECMAC (Figure 8(b)) insulin response models, it is evident that the PSECMAC insulin response model produced more preferable insulin responses due to the general accuracy and consistency of its computed insulin profile.

The GenSoFNN-CRI network, on the other hand, managed to achieve comparable modeling performances

following the adaptive tuning process for both the overeat and the irregular dietary profiles. This is mainly due to the dynamically evolving nature of the GenSoFNN-CRI system that enables it to incrementally adapt its network structure to accomodate newly emerging information. Such a dynamically evolving structure, however, increases the computational complexity of the resultant insulin response model. In addition, GenSoFNN network employs trapezoidal membership functions to define its receptive fields and this reduces the accuracy of its computed output. This is evident from the simulation results presented in Tables 7 and 8 that clearly showed the superior accuracy of the PSECMAC insulin model over its GenSoFNN-CRI counterpart. Lastly, the sets of results from the previous simulations have demonstrated that the proposed PSECMAC insulin response models can be adapted to address the intra- and inter-day variability of the glucose metabolic process of a healthy subject.

# 5 PSECMAC Intelligent Insulin Schedule (Model) for the Regulation of Diabetic Blood Glucose Level Under Non Meal Announcement

The PSECMAC insulin model developed in Section 3 is subsequently applied as a pump controller in a closed-loop glucose regulatory system to regulate the insulin infusion rate to a simulated Type-1 diabetic patient. The control objective of our PSECMAC intelligent insulin schedule (model) is to synthesize the healthy insulin responses in the diabetic subject. That is, the proposed PSECMAC-based glucose regulatory system aims to emulate the physiological process of pancreatic insulin release to drive the insulin profile of the controlled diabetic patient to that of a healthy person. In this study, the GlucoSim simulator for a Type-1 diabetic person is employed as the simulator for the diabetic patient. Similar to the healthy person model, the Type-1 diabetic model of GlucoSim is constructed based on the compartmental modeling of the various organs involved in the human glucose metabolic cycle and their respective interactions. In the Type-1 diabetic model of GlucoSim, however, an intra-peritoneal (IP) insulin injection (to the portal vein) sub-system is included in place of the pancreatic insulin secretion module of the healthy person model. Please refer to [38] for the technical details and a web-based version of the GlucoSim simulator.

As described previously, the work in this section is based on the hypothesis that the rate of insulin secretion by the pancreatic $\beta$-cells in a healthy subject is functionally proportional to the serum insulin concentration measured from time to time. This insulin response, in turn, is derived from the observed glucose fluctuations due to the food disturbances. The proposed insulin pump control module for the closed-loop glucose-insulin regulatory system therefore consists of two sub-systems. They are: (1) the PSECMAC insulin response model; and (2) the interface to the GlucoSim Type-1 diabetic simulator. In this setup, the PSECMAC insulin model

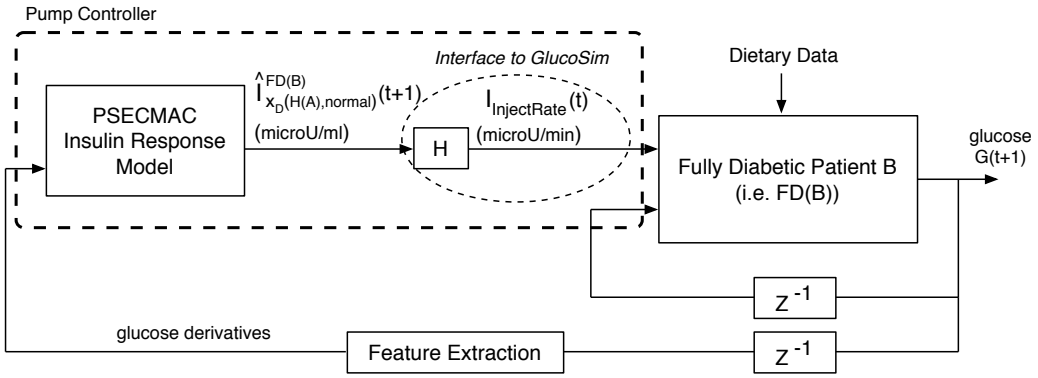


Figure 9: Static closed-loop control setup for PSECMAC-based glucose–insulin regulation

predicts the required future blood insulin concentration based on the glucose indicator values extracted from the metabolic data of the diabetic patient. The simulator interface, on the other hand, serves to transform the predicted future blood insulin concentration (in microU/ml unit) into the equivalent insulin flow rate (in microU/min unit), and to subsequently scale the resultant flow rate to produce the required insulin injection rate. Figure 9 depicts the closed-loop control setup for the PSECMAC-based glucose regulation system.

In the control structure of Figure 9, a fully diabetic patient B (denoted as *FD(B)*) with a BMI similar to that of Subject A is simulated. The diabetic patient model of the GlucoSim simulator accepts, as its inputs, the dietary data and the insulin injection rate as well as the previous metabolic state of the diabetic model. As outputs, the GlucoSim diabetic model computes the current insulin and glucose concentrations in the blood as well as the internal states of the various compartments in the model. All the internal variables are in turn used to compute the next state of the diabetic model. To obtain the appropriate insulin injection rate, the required future insulin response of the diabetic subject *FD(B)* under a particular dietary profile is first computed using the PSECMAC insulin model $\mathfrak{F}^{H(A)}_{\text{normal}}$ of Section 3. The computational output of the PSECMAC insulin model is formalized as eq. (12)

$$\hat{I}^{\text{FD(B)}}_{\text{x}_D,\text{(H(A), normal)}}(t+1) \quad = \quad \mathfrak{F}^{\text{H(A)}}_{\text{normal}}\left(\left\{z^{\text{FD(B)}}_{\text{mces, normal}}(t)\right\}\right) \tag{12}$$

where $\hat{I}^{\text{FD(B)}}_{\text{x}_D,\text{(H(A), normal)}}(t+1)$ denotes the computed insulin requirement of the fully diabetic patient B (i.e. *FD(B)*) for the dietary profile $\text{x}_D \in \{\text{normal}, \text{under}, \text{over}, \text{irregular}\}$ based on the PSECMAC healthy insulin model constructed from the normal diet (i.e. (H(A),normal)); $\left\{z^{\text{FD(B)}}_{\text{mces, normal}}(t)\right\}$ is the set of glucose indicators identified via the MCES feature selection process (see Section 3) after being extracted from the diabetic glucose metabolism data for the normal diet at time $t$; and $\mathfrak{F}^{H(A)}_{\text{normal}}$ refers to the PSECMAC insulin model constructed for the healthy model of Subject A with a normal diet.

Subsequently, the computed insulin response $\hat{I}^{\text{FD(B)}}_{\text{x}_D,\text{(H(A), normal)}}(t+1)$ is applied to the simulator interface

Table 9: The control performances of the PSECMAC-based closed-loop control system for Patient *FD(B)* under the various dietary profiles

| | **PSECMAC-Controlled** | | | **Uncontrolled** | | |
|---|---|---|---|---|---|---|
| **Dietary Profile** | **RMSE** | **PC** | **$\mathbf{PI_1}$** | **RMSE** | **PC** | **$\mathbf{PI_1}$** |
| Normal | 38.915 | 0.6231 | 1.56 | 259.93 | 0.1778 | 0.07 |
| Under | 22.050 | 0.8287 | 3.60 | 203.30 | 0.0957 | 0.05 |
| Over | 64.766 | 0.4832 | 0.73 | 509.19 | 0.2699 | 0.05 |
| Irregular | 53.199 | 0.7727 | 1.43 | 561.48 | 0.2665 | 0.05 |

($H$) to obtain the required insulin injection rate. This is formalized as in eq. (13)

$$\begin{aligned} I_{\text{InjectRate}}(t) &= \mathfrak{H}\left(\hat{I}^{\text{FD(B)}}_{\text{x}_D,\text{(H(A), normal)}}(t+1)\right) \\ &= h \times \hat{I}^{\text{FD(B)}}_{\text{x}_D,\text{(H(A), normal)}}(t+1) \times CR \end{aligned} \tag{13}$$

where $I_{\text{InjectRate}}(t)$ denotes the required injection rate, $\mathfrak{H}$ denotes the transfer function of the simulator interface module (H), $h$ is the scaling factor, and *CR* refers to the conversion rate from the predicted insulin concentration (microU/ml) to the insulin flow rate (microU/min). The conversion rate (*CR*) is computed as [50] described in eq. (14) where BodyWeight refers to the body weight of the diabetic patient.

$$CR = (9.9314 \times \text{BodyWeight} + 0.6859) \tag{14}$$

A series of control simulations were performed on the normal, under, over and irregular dietary profiles to calibrate the scaling factor $h$ of the proposed PSECMAC-based closed-loop glucose–insulin regulatory system under non-meal announcement. From the simulation results, a scaling factor of $h = 5$ was empirically determined to give the best control performances for all the dietary profiles. Table 9 lists the resultant 4-days control performances of the static closed-loop insulin control system with a scaling factor of $h = 5$ for the various dietary profiles. The control efforts of the static PSECMAC-based insulin regulatory system are benchmarked against those of the healthy model. RMSE denotes the root-mean-squared-error value between the blood glucose level of the controlled diabetic subject (*FD(B)*) and the (desired) blood glucose level of the healthy subject (*H(A)*). The PC value, on the other hand, measures the Pearson correlation coefficient between the blood glucose level of the controlled diabetic and that of the healthy subject. Based on the PC and RMSE values, a performance index $\text{PI}_1$ is computed as in eq. (9).

As a baseline comparison to the observed performances of the static PSECMAC-based glucose control system, the set of metabolic simulations for the different diets is repeated but with no insulin infusion. That is, it is assumed that there is no insulin administration to the diabetic patient model. Hence, the diabetic blood glucose fluctuations observed are due to the carbohydrate intakes and the result of the various insulin-

independent glucose removal mechanisms. The simulation results for the uncontrolled (no insulin infusion) glucose metabolic process of *FD(B)* are presented in Table 9.

As highlighted previously, the objective of the glucose regulatory system proposed in this work is to synthesize the healthy glucose-insulin metabolic dynamics in a diabetic subject. From the simulation results tabulated in Table 9, one can observe that the PSECMAC-based glucose regulatory system has achieved encouraging glucose control performances without meal announcement. This is shown by the good correlations between the controlled (diabetic) and healthy blood glucose levels. The best control performances were achieved for the undereat diet with a Pearson correlation of approximately $82.9\%$, indicating a close fit between the controlled and healthy glucose-insulin dynamics. However, the performances of the PSECMAC-based glucose regulation system are comparatively degraded for the irregular and overeat diets, but are still close to the normoglycemia level. This may be due to the poor accuracy of the PSECMAC insulin response model when applied to the irregular and overeat profiles. The PSECMAC insulin response model employed for the simulations was constructed based on the normal dietary data. As reported in Section 4, the output accuracy of the PSECMAC insulin response model trained on the normal diet tends to degrade when applied to the overeat and the irregular diets. Moreover, due to the highly non-linear characteristics of the glucose metabolic cycle, a small inaccuracy in the insulin infusion schedule may translate to a large disparity in the observed diabetic blood glucose concentrations (as compared to the healthy glucose response).

The simulation results in Table 9, however, have clearly demonstrated the significant impact of the proposed PSECMAC-based glucose regulatory system in achieving an effective control of the diabetic blood glucose levels. The glucose metabolic profile of the diabetic Subject B, if left uncontrolled, has a RMSE of as high as $561$ mg/dl (for the irregular diet) with a maximum correlation of only about $27\%$ to the healthy glucose dynamics. Such a high RMSE value suggests that the patient is experiencing extreme and prolonged episodes of hyperglycemia as illustrated in Figure 10. Figure 10 depicts the 3-days blood glucose levels of the diabetic Subject B (controlled and uncontrolled) for the different dietary profiles as benchmarked to those of a healthy person. Specifically, Figure 10 shows that the diabetic patient suffers from multiple severe hyperglycemia episodes for all the evaluated dietary profiles if there is no control of the blood glucose levels.

The PSECMAC-based glucose regulatory system, on the other hand, has been shown to effect an adequate control of the diabetic blood glucose levels so that the patient achieved glucose levels that are highly comparable to those of a healthy person. In particular, with the help of the PSECMAC-based glucose regulation system, the diabetic patient managed to achieve healthy blood glucose levels for the undereat and normal diets without any meal announcement and the intelligent insulin regulatory regime works on the changes in glucose level. Although the controlled blood glucose responses of the diabetic Subject B for the overeat and irregular diets do not follow closely those of a healthy person, the effectiveness of the proposed closed-loop control structure

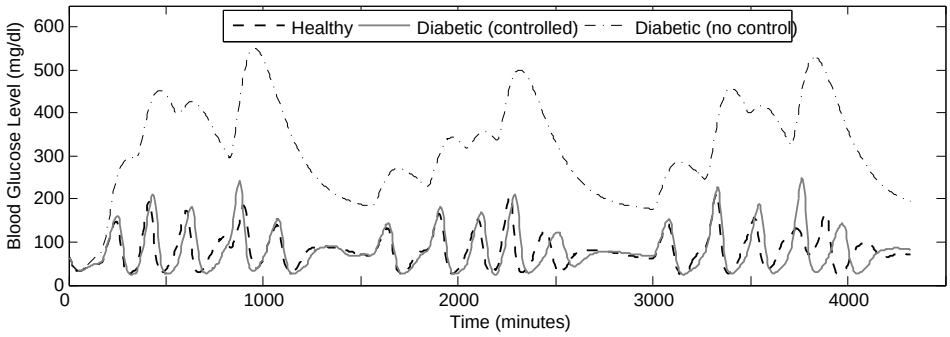


(a) Normal Diet

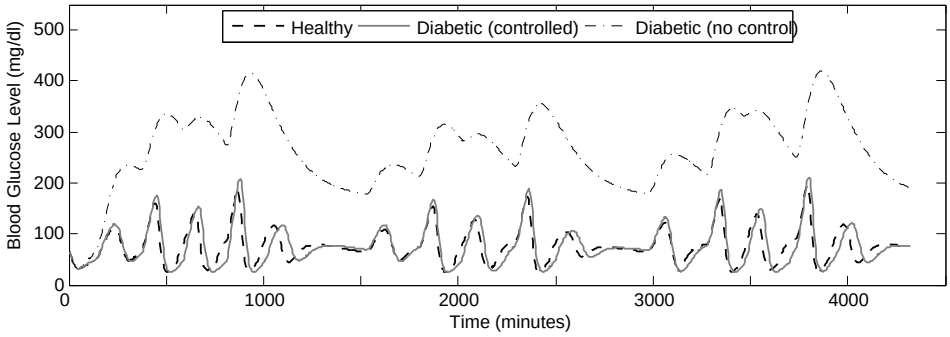


(b) Undereat Diet

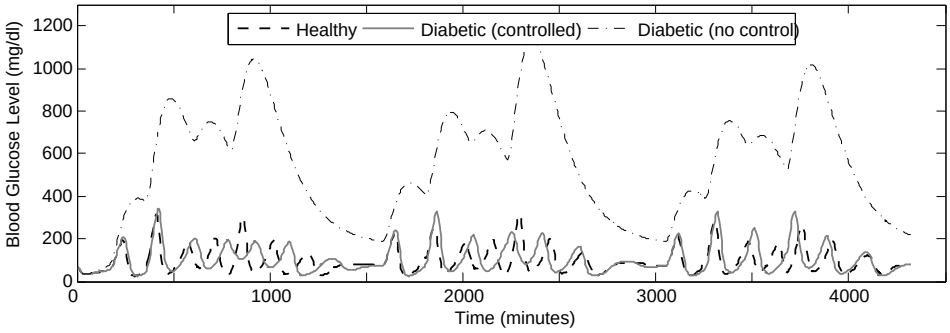


(c) Overeat Diet

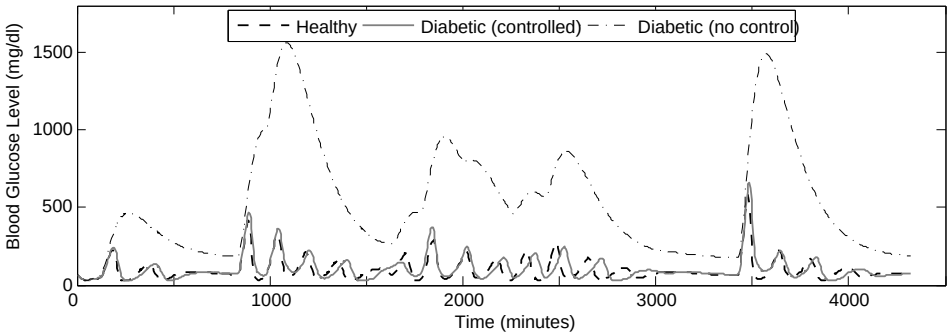


(d) Irregular Diet

Figure 10: 3-days control performances of the PSECMAC intelligent insulin schedule for Patient *FD(B)* under the various dietary profiles

Table 10: The profile of the simulated diabetic Patient *FD(C)* and Patient *FD(D)*

| **Attributes** | **Patient** *FD(C)* | **Patient** *FD(D)* |
|---|---|---|
| Sex | Male | |
| Age | 40 years old | |
| Race | Asian | |
| Height | 1.70 m | |
| Lifestyle | Typical office worker with moderate physical activities such as walking briskly, leisure cycling and swimming. | |
| Weight | 58 kg | 52 kg |
| BMI | 20 | 18 |
| RDA | 323.9 g | 308.5 g |

in maintaining the normoglycemia state of the diabetic patient is clearly reflected in the fast control response time in bringing down the elevated blood sugar levels.

Subsequently, to evaluate the empirical performance of the proposed PSECMAC insulin schedule (model) when it is employed to regulate the blood glucose levels of patients with different metabolic rates, two new diabetic patients (referred to as Patient *FD(C)* and Patient *FD(D)* respectively) that belong to the same subject group as Patient *FD(B)* were simulated. The respective subject profiles of Patient *FD(C)* and Patient *FD(D)* are listed as Table 10. These two newly-created patient profiles are similar to that of Subject A except for the variations in the body weights and thus the resultant BMIs. Based on the respective recommended daily carbohydrate allowance (RDA) of Patient *FD(C)* and Patient *FD(D)*, the meal profiles of each patient for all the four evaluated dietary scenarios (i.e. normal, under, over and irregular diets) were generated using the rules listed in Table 2 of Section 3.1.

The set of glucose control experiments performed using Patient *FD(B)* described above is subsequently repeated for both Patient *FD(C)* and Patient *FD(D)*. That is, the trained PSECMAC insulin schedule (model) is employed to regulate the continuous insulin infusion rates for both patients using the closed-loop glucose-insulin control setup of Figure 9. The blood glucose regulation performances of the PSECMAC-based closed-loop control system for both patients under the various dietary scenarios evaluated is summarized as Table 11. Figures 11 and 12 illustrate respectively the observed blood glucose fluctuations for Patient *FD(C)* and Patient *FD(D)* when there is no insulin infusion and when the PSECMAC-based closed loop insulin infusion system is applied.

From the tabulated results of Table 11 and the plots shown in Figures 11 and 12, one can observe that the diabetic blood glucose levels of the newly simulated patients are well regulated and the quality of control for both Patient *FD(C)* and Patient *FD(D)* are highly comparable to that achieved for Patient *FD(B)*. The simulation results have therefore successfully demonstrated the robustness of our proposed approach in addressing the metabolic biodiversity of diabetic patients from the same subject group and also further reinforced the ef-

Table 11: The control performances of the PSECMAC-based closed-loop control system for Patient *FD(C)* and Patient *FD(D)* under the various dietary profiles (Note: N=Normal, U=Under, O=Over and I=Irregular)

| | **Patient *FD(C)*** | | | | | | **Patient *FD(D)*** | | | | | |
|---|---|---|---|---|---|---|---|---|---|---|---|---|
| | **PSECMAC-Controlled** | | | **Uncontrolled** | | | **PSECMAC-Controlled** | | | **Uncontrolled** | | |
| **Diet** | **RMSE** | **PC** | $\mathbf{PI_1}$ | **RMSE** | **PC** | $\mathbf{PI_1}$ | **RMSE** | **PC** | $\mathbf{PI_1}$ | **RMSE** | **PC** | $\mathbf{PI_1}$ |
| N | 39.323 | 0.7079 | 1.76 | 323.44 | 0.1807 | 0.06 | 34.188 | 0.7125 | 2.02 | 288.65 | 0.2236 | 0.08 |
| U | 23.386 | 0.8150 | 3.34 | 223.67 | 0.1424 | 0.06 | 14.661 | 0.9063 | 5.77 | 204.56 | 0.1678 | 0.08 |
| O | 53.691 | 0.5053 | 0.92 | 421.67 | 0.2184 | 0.05 | 54.418 | 0.5495 | 0.99 | 451.15 | 0.2388 | 0.05 |
| I | 50.205 | 0.7769 | 1.52 | 513.12 | 0.2947 | 0.06 | 49.114 | 0.7282 | 1.45 | 457.05 | 0.2832 | 0.06 |

fectiveness of the proposed PSECMAC intelligent insulin schedule when employed to realize the closed-loop regulation of blood glucose using the no meal announcement method.

# 6 Conclusions

The key to a successful management of diabetes is to maintain long term near-normoglycemia of the diabetic patient. The current protocol and standard of diabetes treatment is largely inadequate due to the following reasons: (1) the de-facto therapy of daily discrete insulin injections for blood glucose control encountered suboptimal therapeutic outcomes as it is difficult to achieve near-normal blood glucose levels via an open-loop control; (2) a majority of the existing closed-loop insulin regulatory systems rely on static mathematical models of the human glucose metabolic process that are often ill-equipped to address the metabolic bio-diversity of the diabetic patients; (3) the currently adopted glucose metabolic model do not account for the intra- and inter-day variability in the metabolic process of the individual patient; and (4) the prior meal announcement in prevailing regimes for diabetes management has substantial drawback due to non-compliant and ill-discipline of the patients.

In this paper, a novel approach to the management of diabetes that addresses the above-mentioned problems was proposed. The developed PSECMAC intelligent insulin schedule (model) aims to emulate the biological process of metabolic insulin secretion by the pancreatic $\beta$-cells in a healthy person and to subsequently reproduce this healthy insulin response in a diabetic patient. The PSECMAC intelligent insulin schedule (model) requires no prior meal announcement and models the healthy insulin response based solely on the observed plasma glucose fluctuations. In the simulations, four types of dietary profiles (i.e. normal, under, over and irregular) were created to simulate the intra- and inter-day variability in the meal intakes of the healthy and diabetic subjects. The PSECMAC insulin schedule is then evaluated on the different dietary profiles to investigate the modeling performances of the proposed insulin response model. The evaluation results has demonstrated that the PSECMAC insulin response model can be adapted to suit the intra- and inter-day variability in the

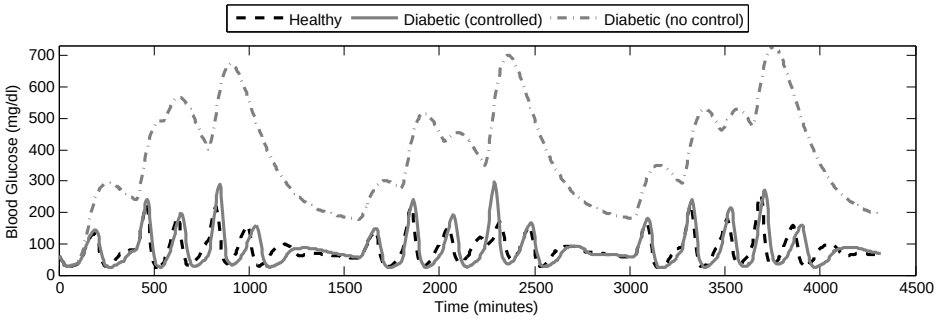


(a) Normal Diet

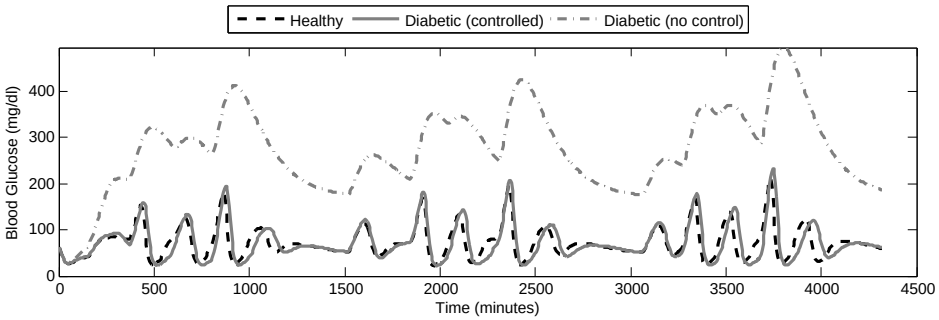


(b) Undereat Diet

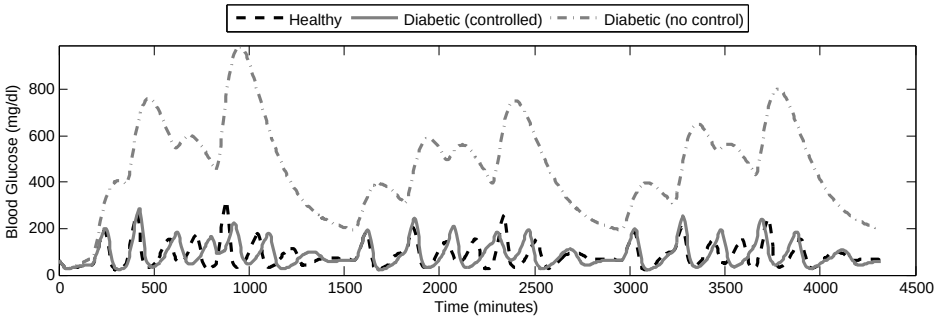


(c) Overeat Diet

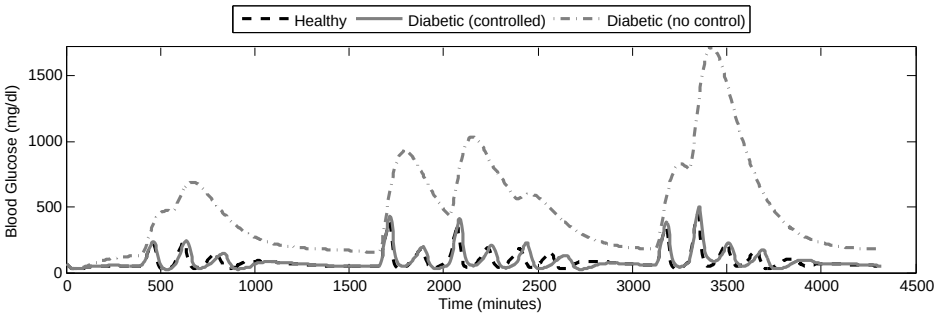


(d) Irregular Diet

Figure 11: 3-days control performances of the PSECMAC intelligent insulin schedule for Patient *FD(C)* under the various dietary profiles

glucose metabolic process of a healthy subject. Subsequently, the PSECMAC intelligent insulin schedule is employed in a closed-loop glucose control system to regulate the diabetic blood glucose level without meal announcement. The preliminary results on a group of simulated Type-1 diabetic patients further established the

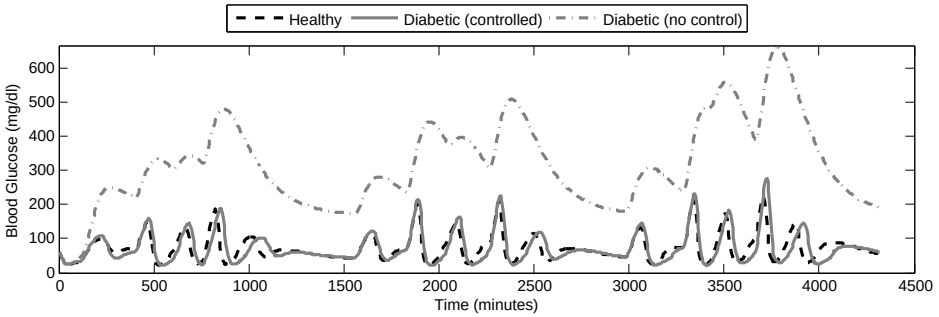


(a) Normal Diet

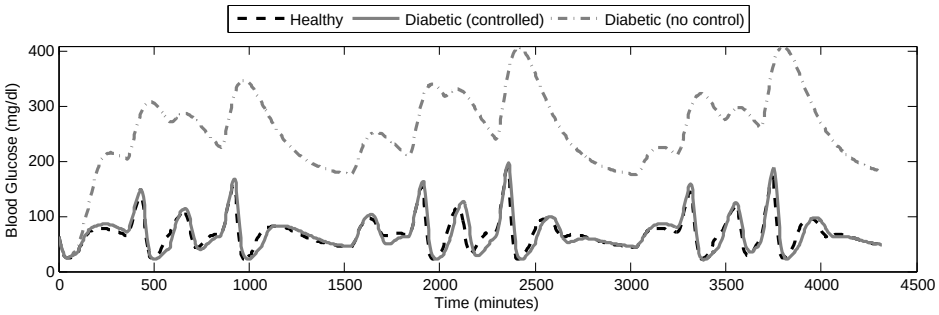


(b) Undereat Diet

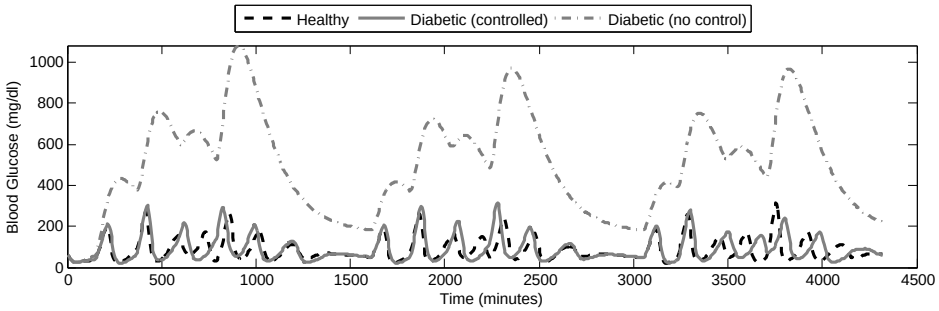


(c) Overeat Diet

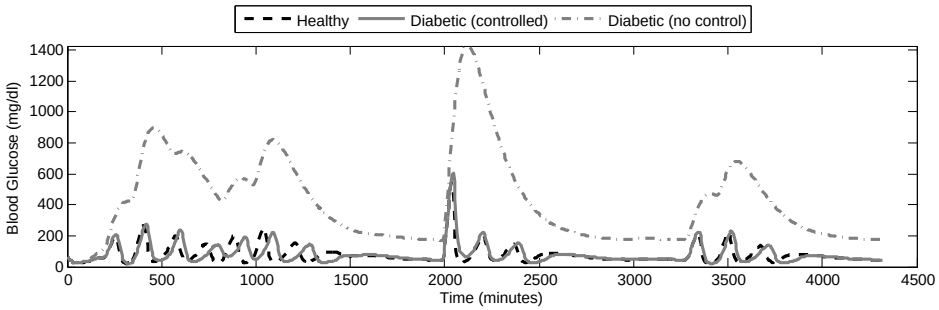


(d) Irregular Diet

Figure 12: 3-days control performances of the PSECMAC intelligent insulin schedule for Patient *FD(D)* under the various dietary profiles

PSECMAC intelligent insulin schedule (model) as a highly promising solution for the personalized management of diabetes and the patient no longer need to announce the meals to the insulin regulatory system. As part of the future work toward this direction, research effort is currently directed at developing an adaptive tuning

strategy for the online updating of the PSECMAC intelligent insulin schedule to create a truly personalized closed-loop glucose-insulin regulatory system. Such an adaptive closed-loop system will allow for optimal therapeutic effectiveness to address the various limitations of existing treatment regimes and enables a diabetic patient to live an active lifestyle.

# References

[1] R. J. Rubin, W. M. Altman, and D. N. Mendelson, "Health care expenditures for people with diabetes mellitus," *Journal of Clinical Endocrinology and Metabolism*, vol. 78, pp. 809A–809F, 1992.

[2] American Diabetes Association, "Economic costs of diabetes in the U.S. in 2002," *Diabetes Care*, vol. 269, no. 3, pp. 917–932, 2003.

[3] Diabetes Control and Complication Trial, "Diabetes control and complication trial (DCCT): The effect of intensive treatment of diabetes in the development and progression of long-term complications in insulin-dependent diabetes mellitus," *The New England Journal of Medicine*, vol. 329, pp. 977–986, 1993.

[4] ——, "The effect of intensive treatment of diabetes in the development and progression of long-term complications in insulin-dependent diabetes mellitus," *Diabetes Care*, vol. 18, pp. 1468–1478, 1995.

[5] L. Fletcher, G. Hraban, P. Huang, B. Srinivasan, and R. Venook, "Feasibility of an implanted, closed-loop, blood-glucose control device," *Immunology*, vol. 230, 2001.

[6] R. Hovorka, "Management of diabetes using adaptive control," *International Journal on Adaptive Control and Signal Processing*, vol. 19, pp. 309–325, 2005.

[7] L. M. Schetky, P. Jardine, and F. Moussy, "A closed loop implantable artificial pancreas using thin film nitinol mems pumps," *Proceedings of International Conference on Shape Memory and Superelastic Technologies (SMST-2003)*, 2003.

[8] M. E. Fisher, "A semiclosed-loop algorithm for the control of blood glucose levels in diabetics," *IEEE Transaction on Biomedical Engineering*, vol. 38, no. 1, pp. 57–61, 1991.

[9] R. L. Ollerton, "Application of optimal control theory to diabetes mellitus," *International Journal of Control*, vol. 50, pp. 2503–22, 1989.

[10] J. T. Sorensen, "A physiologic model of glucose metabolism in man and its use to design and assess improved insulin therapies for diabetes," Ph.D. dissertation, Departement of Chemical Engineering, MIT, 1985.

[11] M. Eren-Oruklu, A. Cinar, L. Quinn, and D. Smith, "Estimation of future glucose concentrations with subject-specific recursive linear models," *Diabetes Technology and Therapeutics*, vol. 11, pp. 243–253, 2009.

[12] A. Makroglou, J. Li, and Y. Kuang, "Mathematical models and software tools for the glucose-insulin regulatory system and diabetes: An overview," *Applied Numerical Mathematics*, vol. 56, pp. 559–573, 2006.

[13] A. De Gaetano and O. Arino, "Mathematical modeling of the intravenous glucose tolerance test," *Journal of Mathematical Biology*, vol. 40, pp. 136–168, 2000.

[14] V. Tresp, T. Briegel, and J. Moody, "Neural network models for the blood glucose metabolism of a diabetic," *IEEE Transactions on Neural Networks*, vol. 10, no. 5, pp. 1204–1213, 1999.

[15] R. S. Parker, F. J. Doyle III, and N. A. Peppas, "A model-based algorithm for blood glucose control in type-1 diabetic patient," *IEEE Transactions on Biomedical Engineering*, vol. 46, pp. 148–157, 1999.

[16] R. Hovorka, V. Canonico, L. J. Chassin, U. Haueter, M. Massi-Benedetti, M. O. Federici, T. R. Pieber, H. C. Schaller, L. Schaupp, T. Vering, and M. E. Wilinska, "Nonlinear model predictive control of glucose concentration in subjects with type-1 diabetes," *Physiological Measurement*, vol. 25, pp. 905–920, 2004.

[17] B. W. Bequette, "A critical assessment of algorithms and challenges in the development of a closed-loop artificial pancreas," *Diabetes Technology and Therapeutics*, vol. 7, pp. 28–47, 2005.

[18] F. M. Ashcroft and S. J. H. Ashcroft, *Insulin: Molecular Biology to Pathology*. New York: Oxford University Press, 1992.

[19] D. Porte Jr., D. G. Baskin, and M. W. Schwartz, "Insulin signaling in the central nervous system," *Diabetes*, vol. 54, no. 5, pp. 1264–1276, 2005.

[20] M. W. Schwartz and D. Porte Jr., "Diabetes, obesity and the brain," *Science*, vol. 307, pp. 375–379, 2005.

[21] K. Prank, C. Jurgens, A. von zur Muhlen, and G. Brabant, "Predictive neural networks for learning the time course of blood glucose levels from complex interaction of counterregulatory hormones," *Neural Computation*, vol. 10, pp. 941–953, 1998.

[22] R. Bellazzi, G. Nucci, and C. Cobelli, "The subcutaneous route to insulin-dependent diabetes therapy," *IEEE Engineering in Medicine and Biology*, vol. 20, no. 1, pp. 54–64, 2001.

[23] R. S. Parker, F. J. Doyle III, and N. A. Peppas, "The intravenous route to insulin-dependent diabetes therapy," *IEEE Engineering in Medicine and Biology*, vol. 20, no. 1, pp. 65–73, 2001.

[24] S. D. Teddy, C. Quek, and E. M.-K. Lai, "PSECMAC: A novel self-organizing multi resolution associative memory architecture," *IEEE Transactions on Neural Networks*, vol. 19, no. 4, pp. 689–712, 2008.

[25] E. R. Kandel, J. H. Schwartz, and T. M. Jessell, *Principles of Neural Science, 4th Edition*. McGraw-Hill, Health Professions Division, 2000.

[26] W. T. Thach, "What is the role of the cerebellum in motor learning and cognition?" *Trends in Cognitive Sciences*, vol. 27, no. 9, pp. 331–337, 1998.

[27] F. A. Middleton and P. L. Strick, "Cerebellar output: Motor and cognitive channels," *Trends in Cognitive Sciences*, vol. 27, no. 9, pp. 348–354, 1998.

[28] ——, "The cerebellum: An overview," *Trends in Cognitive Sciences*, vol. 27, no. 9, pp. 305–306, 1998.

[29] J. S. Albus, "Marr and Albus theories of the cerebellum: Two early models of associative memory," *Proceedings of IEEE COMPCON*, pp. 577–582, 1989.

[30] H. Eichenbaum, *The Cognitive Neuroscience of Memory: An Introduction*. Oxford University Press, 2002.

[31] S. D. Teddy, E. M.-K. Lai, and C. Quek, "Hierarchically clustered adaptive quantization CMAC and its learning convergence," *IEEE Transactions on Neural Networks*, vol. 18, no. 6, pp. 1658–1682, 2007.

[32] ——, "A cerebellar associative memory approach to option pricing and arbitrage trading," *Neurocomputing*, vol. 71, pp. 3303–3315, 2008.

[33] W. L. Tung and C. Quek, "eFSM - a novel online niral-fuzzy semantic memory model," *IEEE Transactions on Neural Networks, in press*, 2009.

[34] R. S. Sherwin, K. J. Kramer, J. D. Tobin, P. A. Insel, J. E. Liljenquist, M. Berman, and R. Andres, "A model of the kinetics of insulin in man," *Journal of Clinical Investigation*, vol. 53, pp. 1481–1492, 1974.

[35] G. Toffolo, M. Campioni, R. Basu, R. A. Rizza, and C. Cobelli, "A minimal model of insulin secretion and kinetics to assess hepatic insulin extraction," *American Journal of Physiology, Endocrinology and Metabolism*, vol. 290, pp. E169–E176, 2006.

[36] W. R. Puckett, "Dynamic modeling of diabetes mellitus," Ph.D. dissertation, Departement of Chemical Engineering, Wisconsin-Madison, 1992.

[37] U. Fischer, H. Hommel, H. D. Gottschling, P. Heinke, and E. Jutzi, "Estimation of pancreatic iri output rate and its relation to glucose tolerance in normal anaesthetized dogs," *Diabetologia*, vol. 11, pp. 291–299, 1975.

[38] GlucoSim, "GlucoSim: A web-based educational simulation package for glucose-insulin levels in the human body," *Illinois Institute of Technology, http://216.47.139.198/glucosim/gsimul.html*, Online.

[39] C. Erzen, G. Birol, and A. Cinar, "Development and implementation of an educational simulator: GLUCOSIM," *Chemical Engineering Education*, vol. 37, no. 4, pp. 300–305, 2003.

[40] A. Cinar, "A. web-based simulations for dynamic variations in blood glucose concentration of patients with type 1 diabetes," in *E. Opara (Ed.) Nutrition and Diabetes: Pathophysiology and Management*. CRC/Taylor and Francis Press, Boca Raton, FL, 2005, pp. 281–300.

[41] HPBSg, "Health promotion board singapore," *http://www.hpb.gov.sg*, Online.

[42] K. Quah and C. Quek, "MCES: A novel monte carlo evaluative selection approach for objective feature selections," *IEEE Transactions on Neural Networks*, vol. 18, no. 2, pp. 431–448, 2007.

[43] J. S. Albus, "A new approach to manipulator control: The cerebellar model articulation controller (CMAC)," *Journal of Dynamic Systems, Measurement, and Control. Trans. ASME*, pp. 220–227, 1975.

[44] ——, "Data storage in cerebellar model articullation controller (CMAC)," *Journal of Dynamic Systems, Measurement, and Control. Trans. ASME*, pp. 228–233, 1975.

[45] J. Sim, W. L. Tung, and C. Quek, "FCMAC-Yager: A novel Yager inference scheme based fuzzy CMAC," *IEEE Transactions on Neural Networks*, vol. 17, no. 6, pp. 1394–1410, 2006.

[46] W. L. Tung, C. Quek, and P. Y. K. Cheng, "GenSo-EWS: A novel neural-fuzzy based early warning system for predicting bank failures," *Neural Networks*, vol. 17, no. 4, pp. 567–587, 2004.

[47] WEKA, "WEKA 3: Data mining software in java," *The University of Waikato, http://www.cs.waikato.ac.nz/ml/weka/*, Online.

[48] G. A. Larsen, S. Cetinkunt, and A. Donmez, "CMAC neural network control for high precision motion control in the presence of large friction," *Journal of Dynamic Systems, Measurement, and Control*, vol. 117, pp. 415–420, 1995.

[49] S. Ku, G. A. Larsen, and S. Cetinkunt, "Fast servo control for ultra-precision machining at extremely low feed rates," *Mechatronics*, pp. 381–393, 1998.

[50] K. B. Bischoff, "Physiological pharmacokinetics," *Bulletin of Mathematical Biology*, vol. 48, no. 3–4, pp. 309–322, 1986.

**Authors' Biographies**

1. 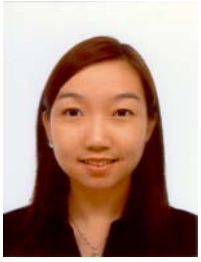 S. D. Teddy

S. D. Teddy received both her B.Eng. (First Class Honors) and Ph.D. degrees in computer engineering from Nanyang Technological University, Singapore, in 2003 and 2008 respectively. She is currently a research fellow with the Data Mining Department of the Institute for Infocomm Research, A*STAR, Singapore. Her current research interests include the cerebellum and its computational models, artificial neural networks, the study of brain-inspired learning memory systems, computational finance, and autonomous control of bio-physiological processes.

2.  C. Quek

C.Quek received the B.Sc. degree in electrical and electronics engineering and the Ph.D. degree in intelligent control from Heriot Watt University, Edinburgh, Scotland. He is an associate professor and a member of the Centre for Computational Intelligence, formerly the Intelligent Systems Laboratory and the Assistant Chair at the School of Computer Engineering, Nanyang Technological University. His research interests include intelligent control, intelligent architectures, AI in education, neural networks, fuzzy neural systems, neurocognitive informatics and genetic algorithms. C.Quek is a Member of IEEE and a member of the IEEE Technical Committee on Computational Finance.

3.  **Edmund M-K. Lai**

**Edmund M-K. Lai** received the B.E.(Hons) and PhD degrees in 1982 and 1991 respectively from the University of Western Australia, both in electrical engineering. He is currently a faculty member of the School of Engineering and Advanced Technology, Massey University in Wellington, New Zealand. Previously he has been a faculty member of the Department of Electrical and Electronic Engineering, The University of Western Australia from 1985 to 1990, the Department of Information Engineering, the Chinese University of Hong Kong from 1990 to 1995, Edith Cowan University in Perth from 1995 to 1998 and the School of Computer Engineering, Nanyang Technological University in Singapore from 1999 to 2006. His current research interests include artificial neural networks, compressed sensing, and information theory.

4.  Ali Cinar

Ali Cinar is a professor of chemical engineering at Illinois Institute of Technology, Vice Provost for Research and Dean of the Graduate College at IIT since 2000 and the director of the Engineering Center for Diabetes Research and Education since 2004. His research specializations include agent-based techniques for modeling, supervision and control of complex and distributed systems, modeling of diabetes, angiogenesis and tissue formation, and automatic control of insulin pumps for patients with diabetes. Dr. Cinar holds a Ph.D. in chemical engineering from Texas A&M University. He is a member of IEEE and fellow of AIChE. He has published two books, over 180 technical papers in refereed journals and conference proceedings. Full list of publications, detailed description of research interests, presentations, and software is available at www.chbe.iit.edu/~cinar